LASER-ASSISTED PLASMA SPECTROMETRY IN THE ANALYSIS OF TECHNOLOGICAL, GEOLOGICAL, ARCHAEOLOGICAL AND ENVIRONMENTAL SAMPLES

Viktor Kanický

Laboratory of Atomic Spectrochemistry,

Division of Analytical Chemistry,

Department of Chemistry,

Faculty of Science

Masaryk University, Brno, Czech Republic

OUTLINE 1

- Principles and instrumentation of laser assisted plasma spectrometry
- Applications
  - Imaging of 2D-distribution of elements
  - Determination of average composition (bulk analysis)

OUTLINE 2

1. What is laser assisted plasma spectrometry?
2. Applications:
    i. technological materials;
    ii. geology;
    iii. archaeology;
    iv. environmental.

What is laser assisted plasma spectrometry?

Laser ablation processes

- Interaction of pulsed (nanosecond, fs) laser focused beam with solids at high laser power density (~10^9 W/cm^2) causes rapid release of material from the surface and near-surface layer – <u>laser ablation</u>
- Laser ablation results from rapid heating of sub-surface volume ⇒ high pressure of vaporized sub–surface material brings about surface layer explosion. Besides, melting occurs.
- Released matter consists of aerosol, vapour, atoms&ions.

Laser ablation processes

- Besides, ambient gas is ionized and forms together with ionized sample microplasma
- Laser radiation is partly absorbed in microplasma ⇒ energy transfer to atoms and ions occurs
- Absorbing microplasma existing for μ-seconds shields sample surface – attenuation of laser beam power applied to a sample – efficiency decreases ⇒ contribution of thermal effects ⇒ undesired melting ⇒ fractionation of elements (boiling temperatures)
- Microplasma existing for μ-seconds in contact with sample heats surface ⇒ undesired melting ⇒ fractionation of elements (boiling temperatures).

Laser ablation processes

- Heating of gas induces shock wave (pressure, acoustic effect), microplasma expands and extinguishes
- Cooling of microplasma causes condensation of vapours into fine aerosol droplets and solidification of liquid droplets into coarse particles ⇒ different composition ⇒ fractionation of elements
- Some particles (coarse, liquid droplets) fall around crater „ejecta“
- Aerosol is possible to transport with carrier gas into ICP with detection either radiation (LA-ICP-OES) or ions (LA-ICP-MS)
- Radiation of analytes in microplasma is measured (LIBS)

Laser ablation

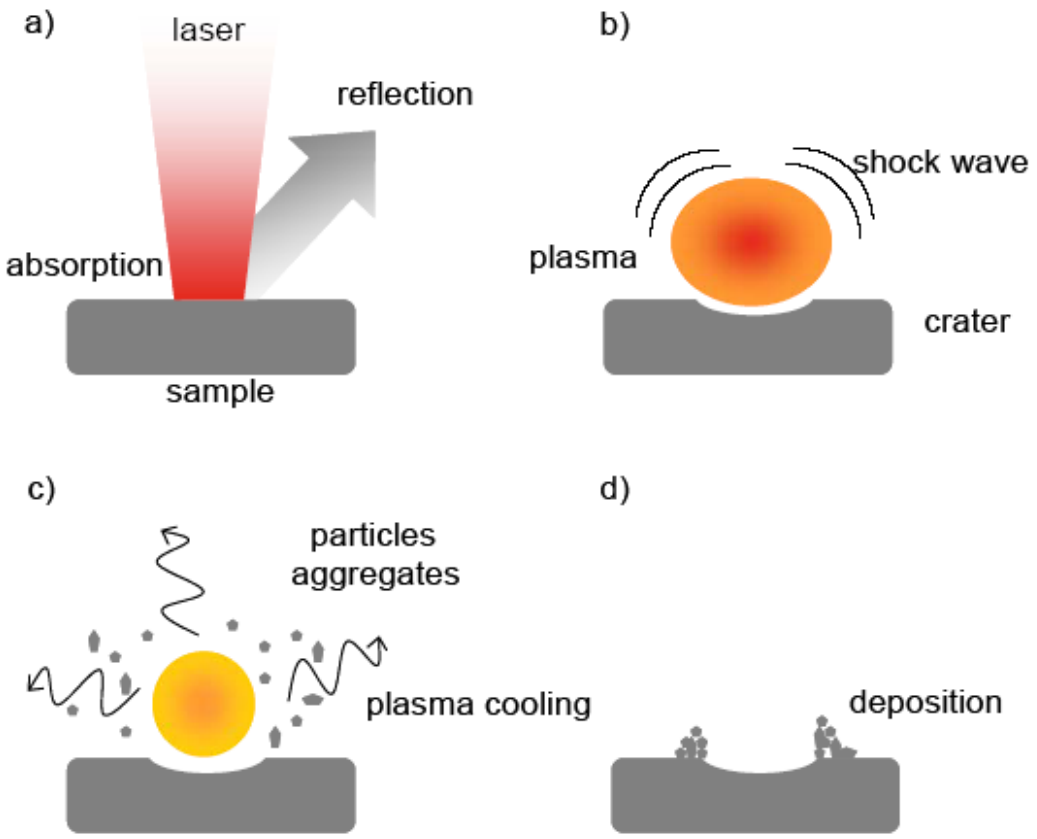

Laser ablation process: a) laser – sample interaction; b) plasma and sample creation; c) plasma cooling effect; d) rim deposition

T. Čtvrtníčková: PhD Dissertation, Masaryk University, 2008

- Laser assisted plasma spectrometry
  - **L**aser **A**blation **I**nductively **C**oupled **P**lasma **M**ass **S**pectrometry: **LA-ICP-MS**
  - **L**aser **A**blation **I**nductively **C**oupled **P**lasma **O**ptical **E**mission **S**pectrometry: **LA-ICP-OES**
  - **L**aser **I**nduced **B**reakdown **S**pectrometry: **LIBS**

Laser Ablation

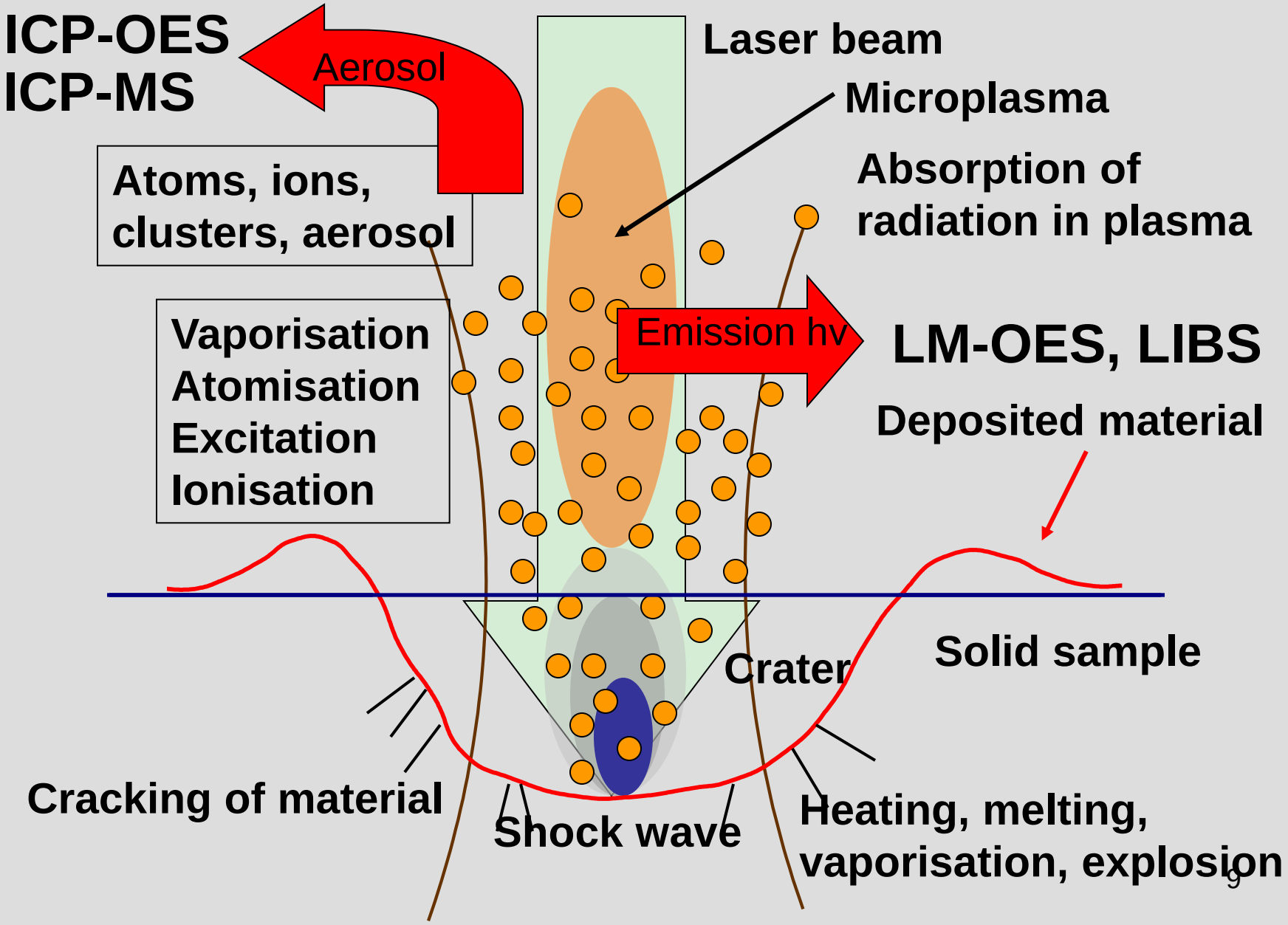

LA-ICP-MS/OES

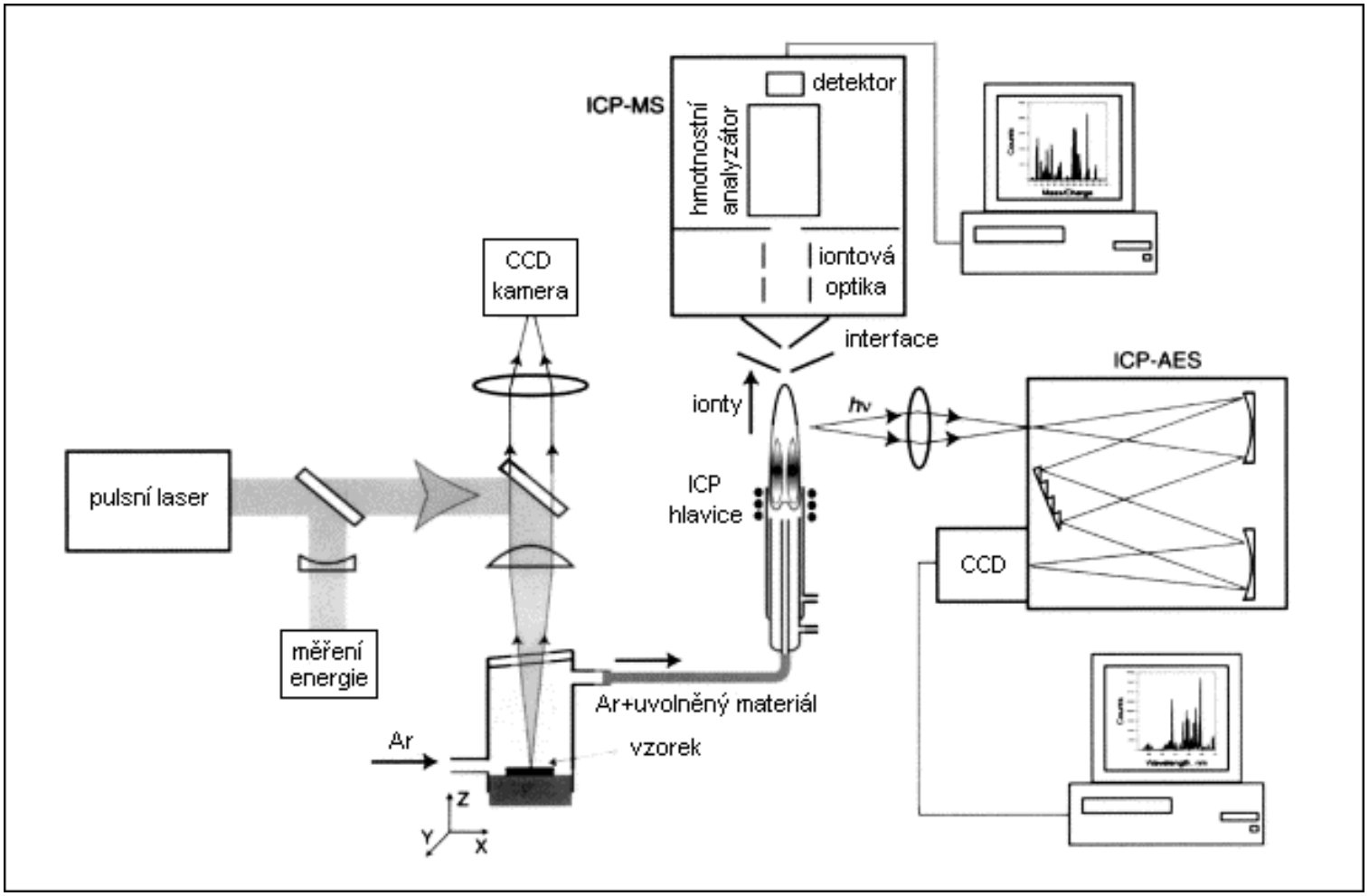

[R.E. Russo, X. Mao, H. Liu, J. Gonzalez, S.S. Mao, Review, Talanta 57 (2002) 425–451]

LA-ICP-MS/OES

ICP discharge ~ ionization source for MS

~ emission source for OES

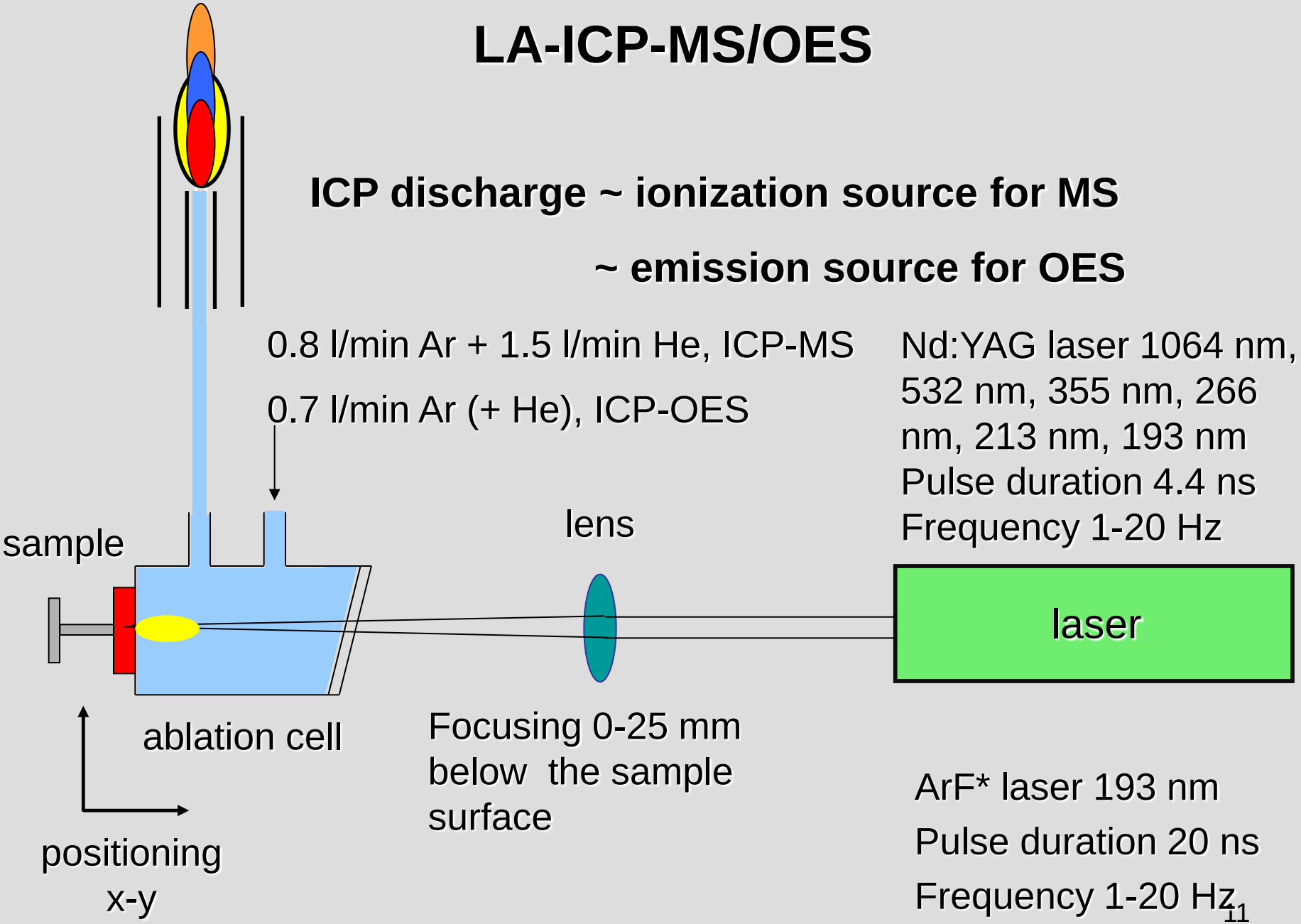

Localized analysis: laser ablation system

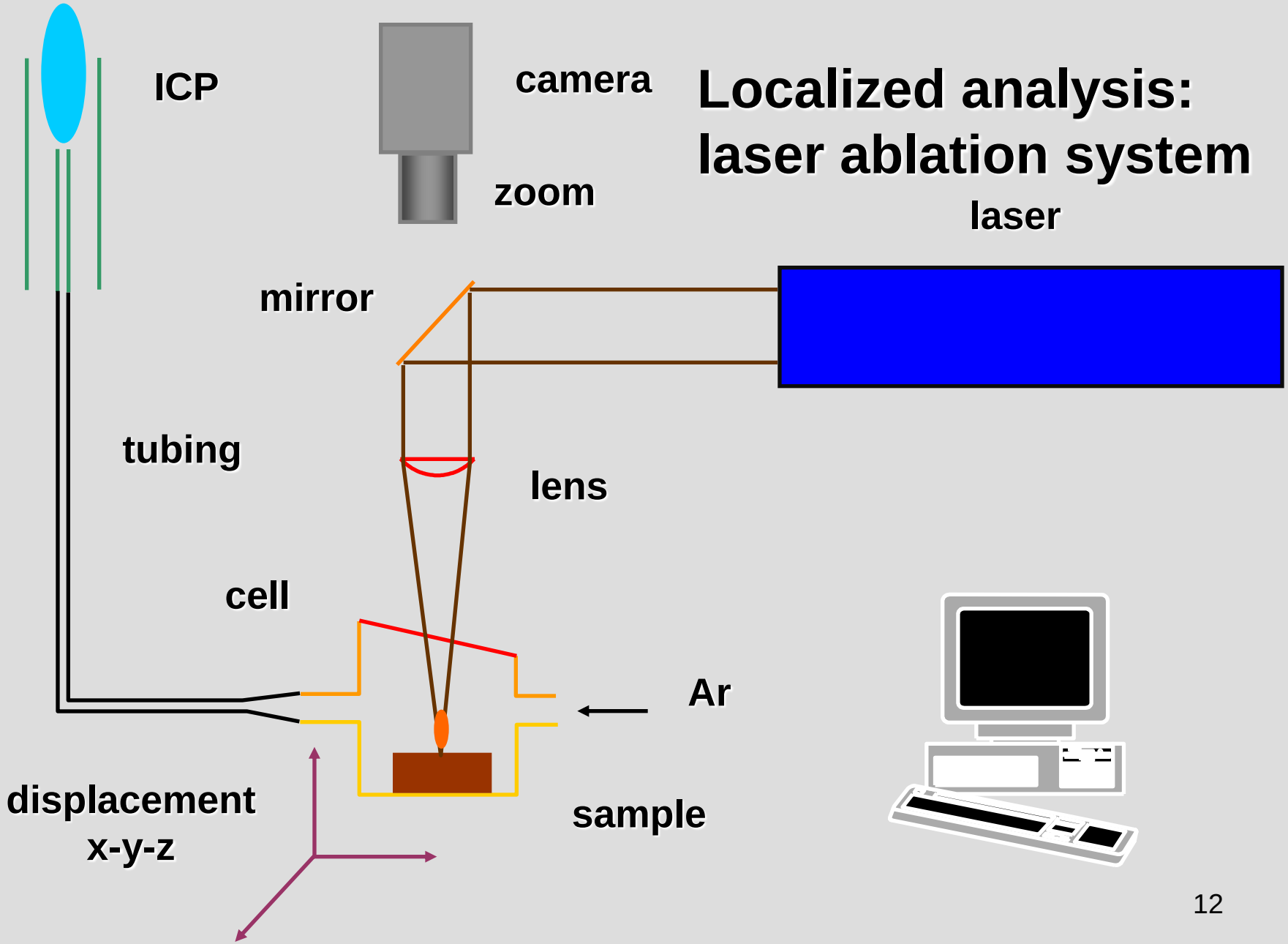

LA-ICP-MS instrumentation
LAS, Masaryk University, Brno

Nd:YAG laser UP-213 (New Wave Resaerch)

213 nm

frequency: 1-20 Hz

pulse: 4.2 ns

spot size 4-300 μm

ICP-MS Agilent 7500ce

generator 27.12 MHz

collision cell

quadrupole mass filter

electron multiplier

LIBS

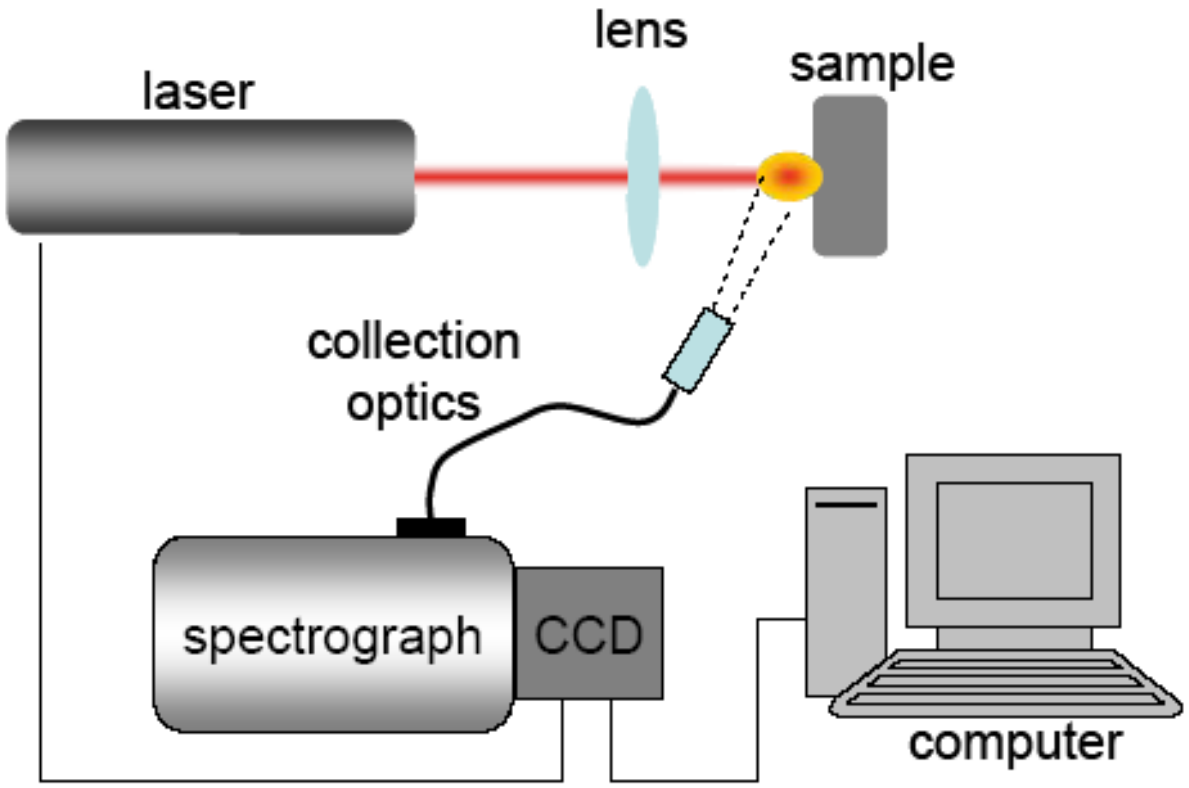

The scheme of LIBS instrumentation

T. Čtvrtníčková: PhD Dissertation, Masaryk University, 2008

LIBS arrangement

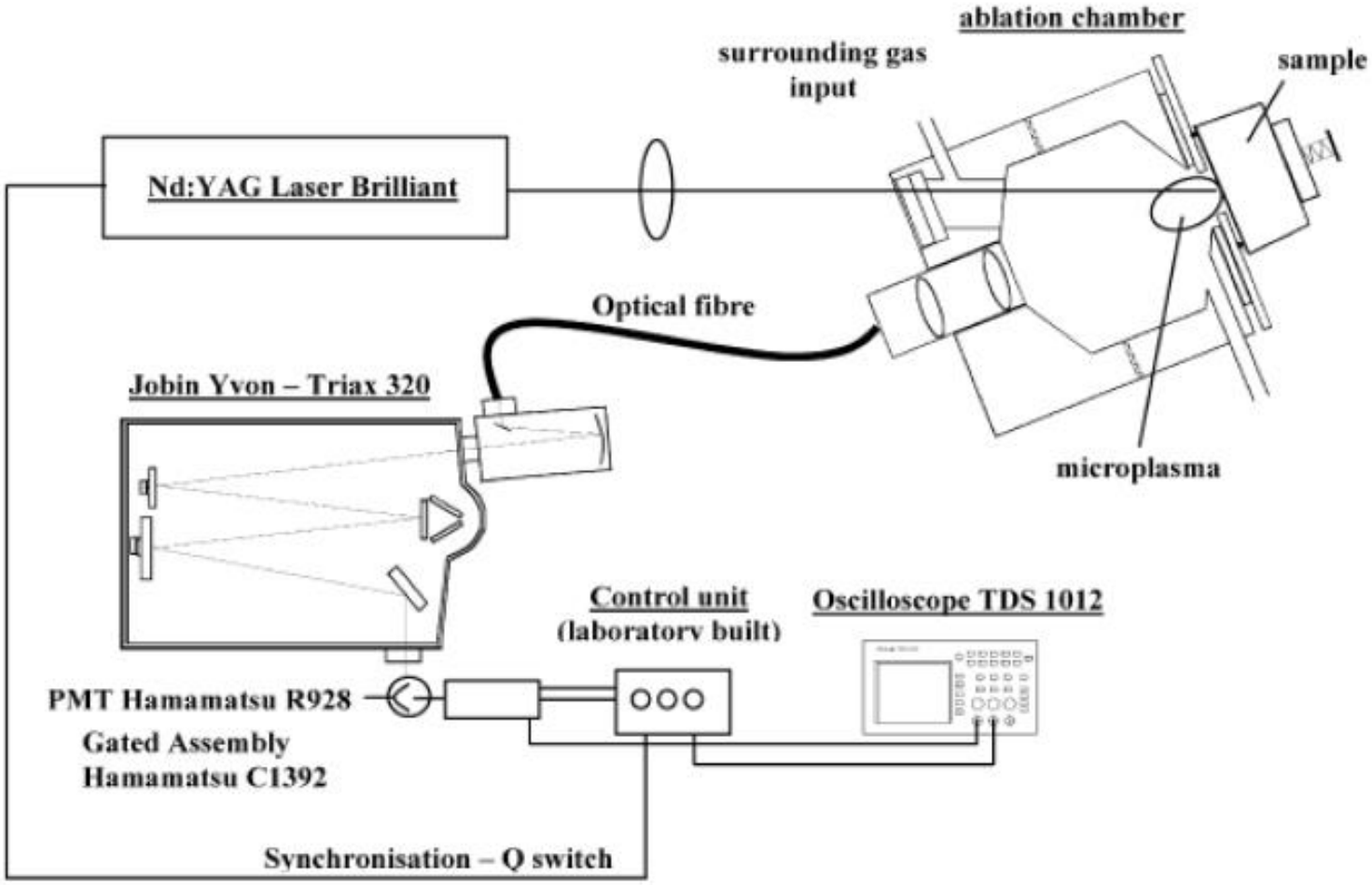

K. Novotný, Masaryk University

LIBS – optimum delay time

Optimum delay time selection from signal and background intensity dependence on delay time, Al (I) 396.152 nm, background 397.5 nm; 266 nm laser (4th harmonics)

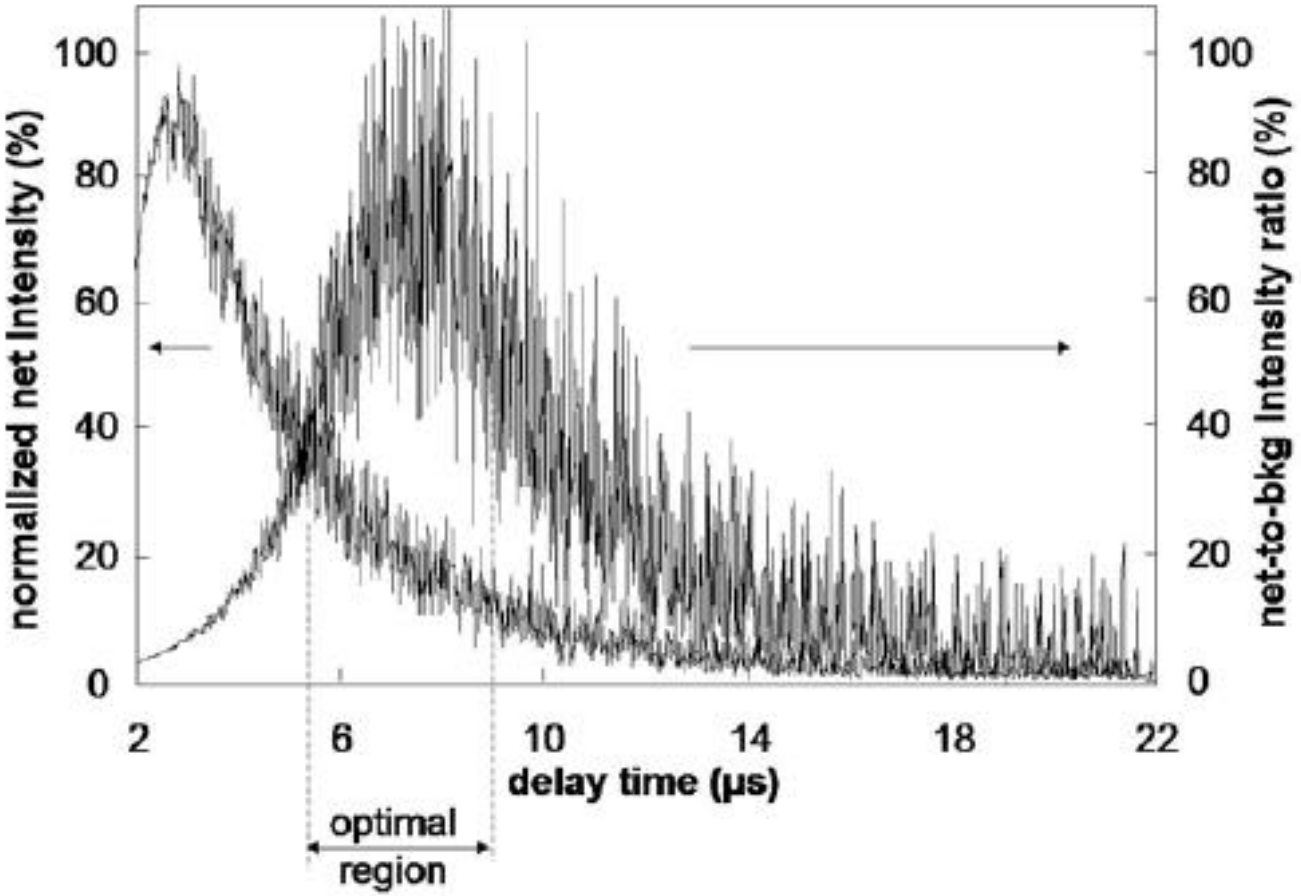

T. Čtvrtníčková: PhD Dissertation, Masaryk University, 2008

Double-pulse LIBS

orthogonal, re-heating mode

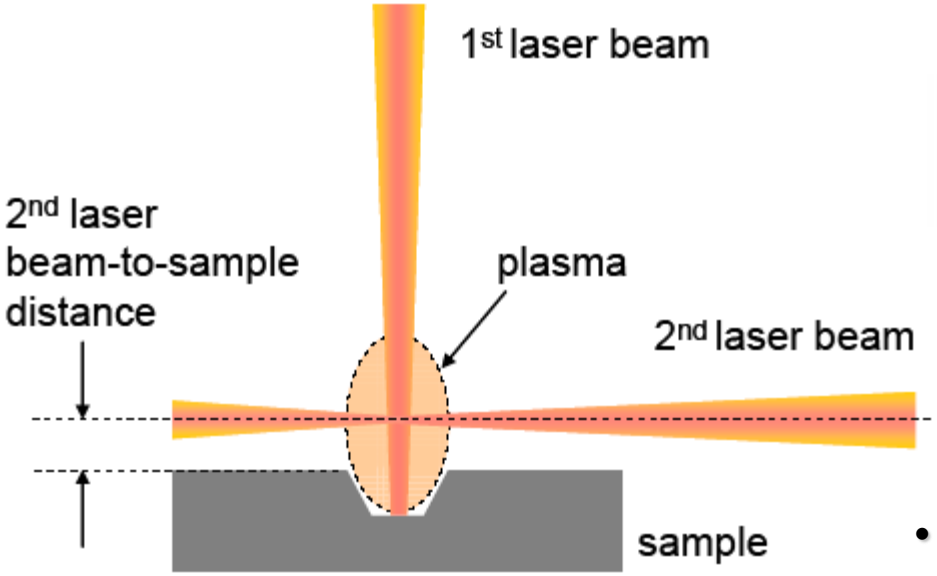

T. Čtvrtníčková: PhD Dissertation, Masaryk University, 2008

K. Novotný: Masaryk University

- monochromator Jobin - Yvon TRIAX, optical fiber,
- CCD Jobin Yvon Horiba,
- gated photomultiplier Hamamatsu

Double pulse LIBS

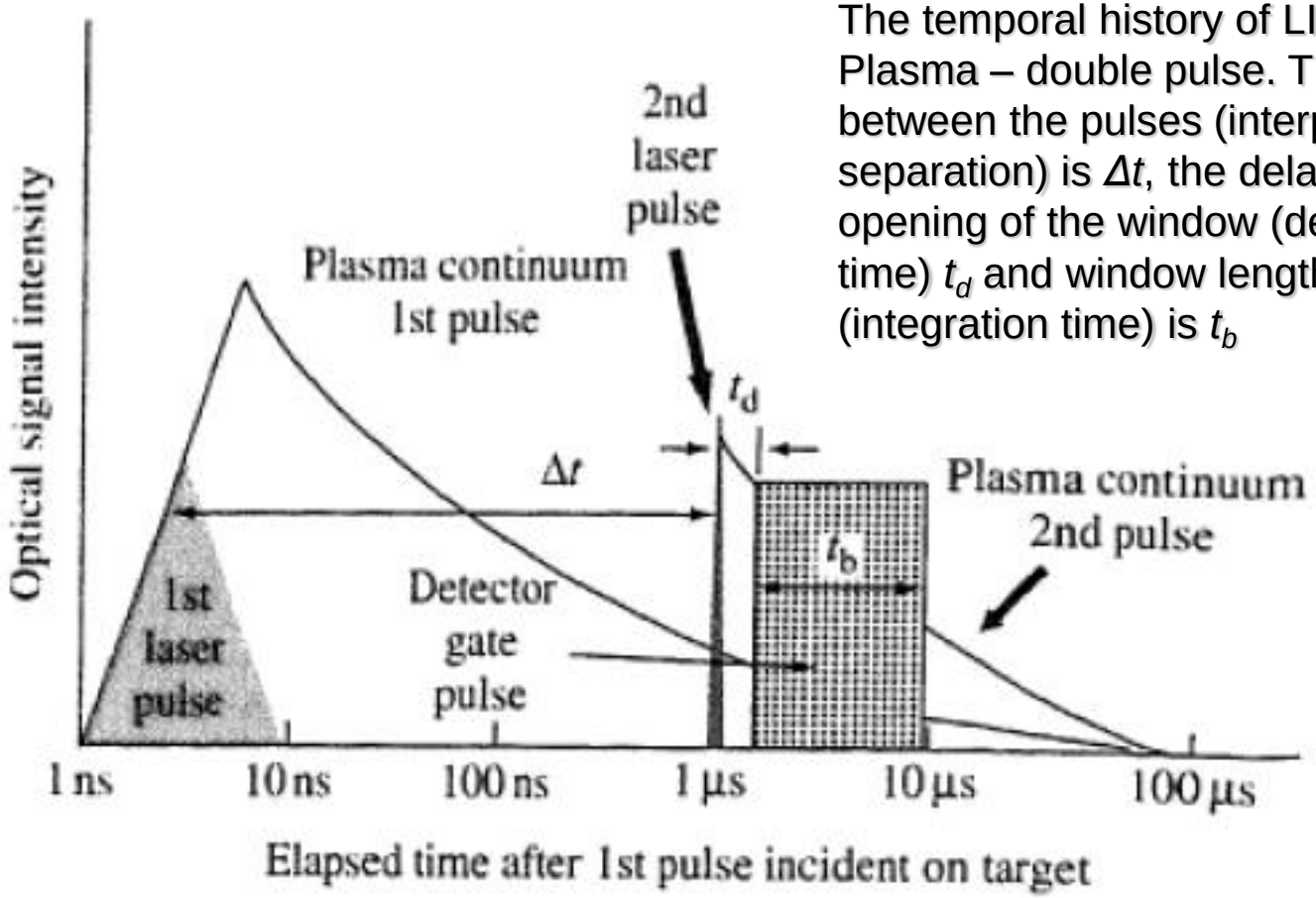

The temporal history of LIBS Plasma – double pulse. The delay between the pulses (interpulse separation) is Δt, the delay to the opening of the window (delay time) t_d and window length (integration time) is t_b

D. Cremers, L.J. Radziemski, Handbook of laser-induced breakdown spectroscopy, John Wiley & Sons, London, 2006.

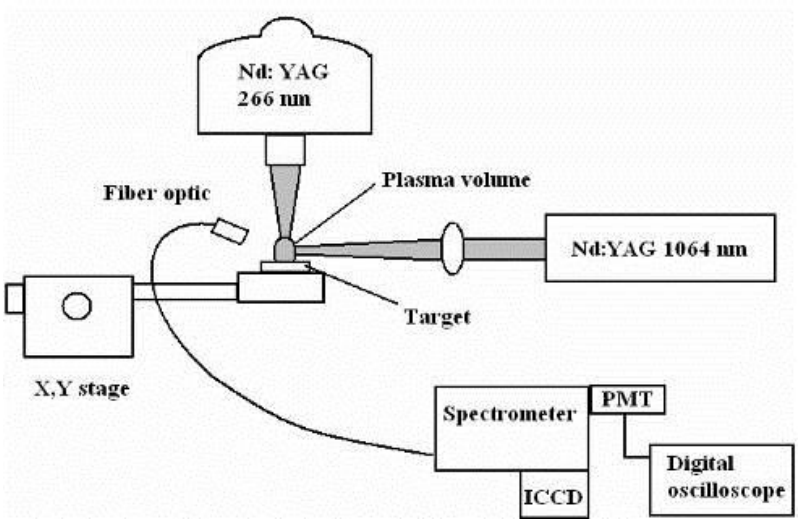

Double–pulse orthogonal configuration in reheating mode

K. Novotný, Masaryk University

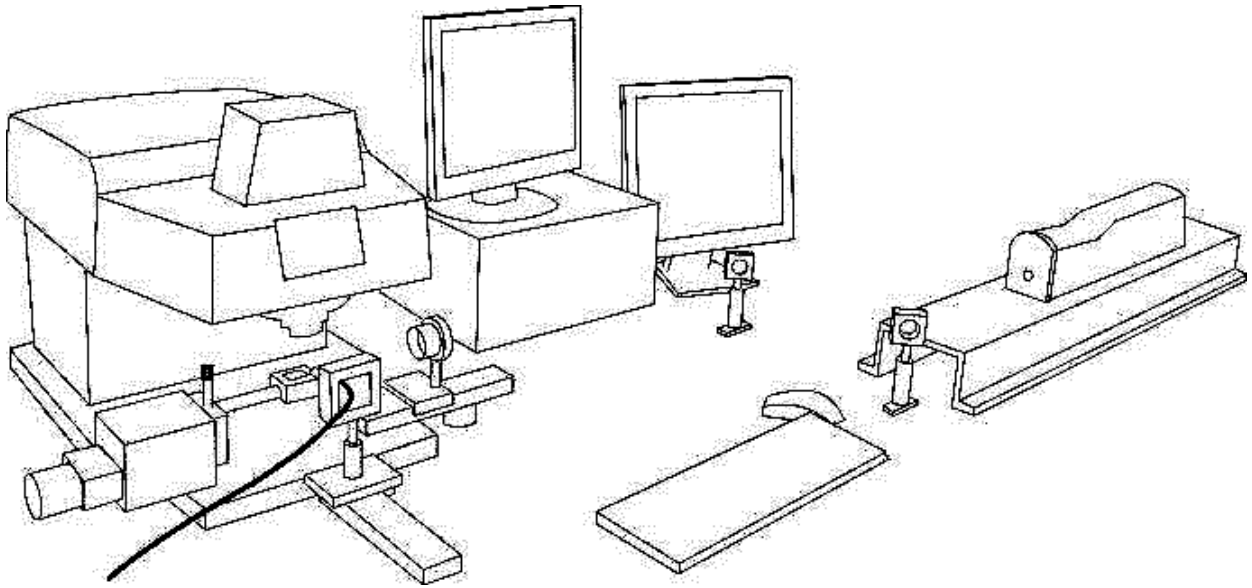


SERIES
Brilliant

Double pulse LIBS

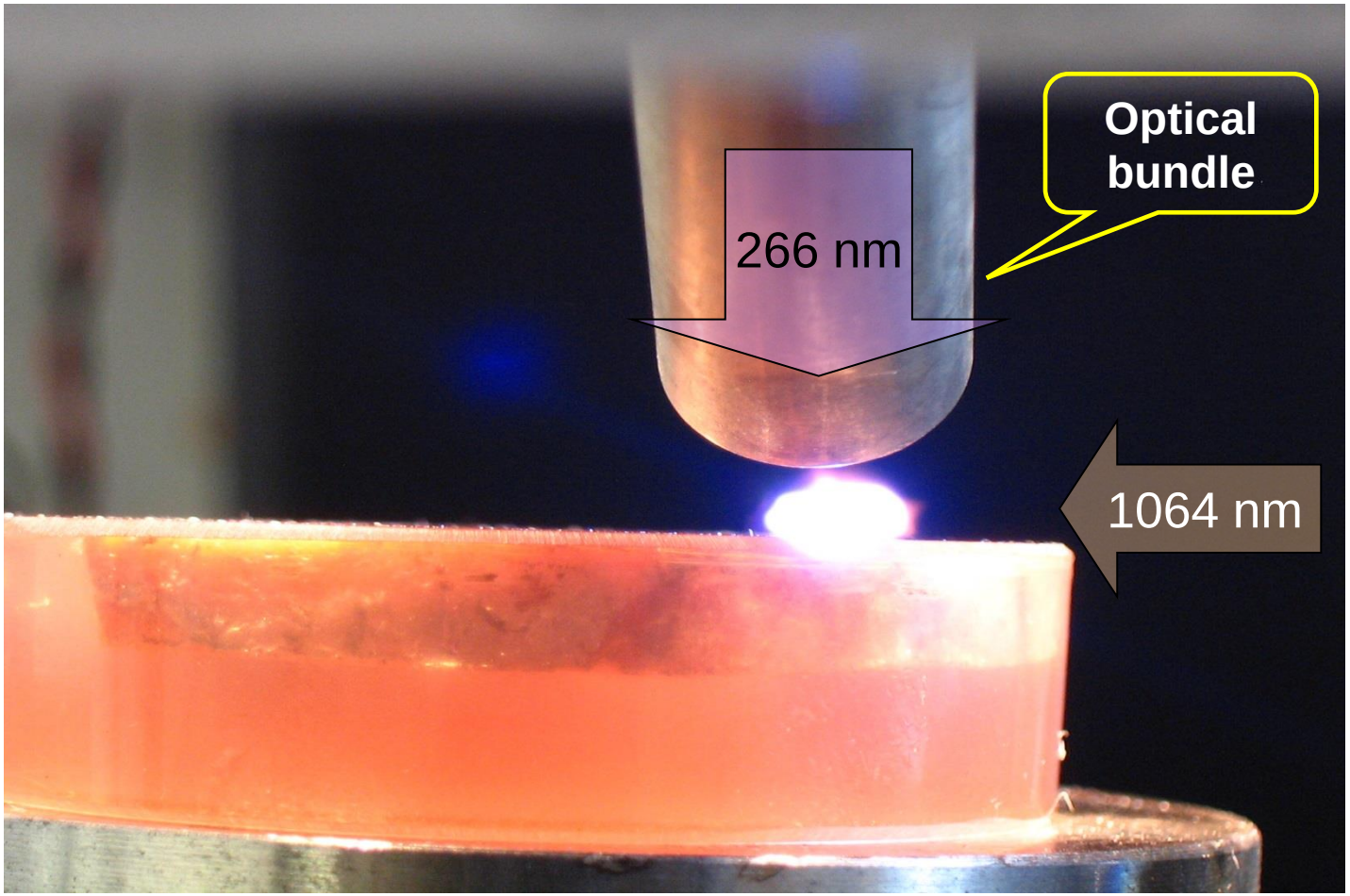

A. Hrdlička, L. Prokeš, V. Konečná, K. Novotný, V. Kanický, V. Otruba

K. Novotný, J. Novotný, J. Kaizer, R. Malina, M. Galiová, V.Otruba, V.K.

Laser-assisted analysis of solids

- Features of laser ablation based techniques
  - Elimination of decomposition for solution analysis
  - Elimination of water, O, N, S, Cl from acids; resulting species cause spectral interferences in ICP-MS
  - Universal: electric conductors, non(semi)conductors
  - Non-destructive: material removing from the area 10 μm^2 to 1mm^2 to the depth cca 0.01-0.1µm/laser pulse
  - 2D-3D „speciation”: preserves information on spatial distribution of elements

Priorities of laser-assisted plasma spectroscopy

1) Analysis of surfaces and coatings: xy - local analysis, microanalysis, areal mapping (mineralogical sections, inhomogeneities in steel)
2) Depth profiling of multi-layer advanced materials or natural structured objects (xyz resolution)
3) Bulk analysis:
   - Compact samples (steel, alloys, glass, ceramics)
   - Powdered samples:
     - pressed pellets with or without a binder,
     - cast pellets with e.g. epoxy resin, polyurethane … ,
     - melted with fusing agents for XRF $\Rightarrow$ cast pearls

Influencing parameters

- Laser wavelength.
- Pulse energy.
- Focus position relative to surface.
- Laser repetition rate.
- Crater diameter/depth (aspect ratio).

Critical parameters of LA

- **Wavelength (UV×IR) *vs* fractionation**
- **Pulse duration (fs×ns) *vs* fractionation**

Features important for particular tasks

- Depth profiling, mapping, local analysis:
  - Laser beam profile, spot size, aspect ratio,
- Bulk analysis:
  - Powders: pellet preparation, cohesion and homogeneity, easy calibration
  - Compacts: no preparation, homogeneity, lack of calibration samples

Effect of laser wavelength

- ✓ Infrared laser: Nd:YAG 1064 nm
  - ✓ Strongly absorbing microplasma, long interaction $\Rightarrow$ thermal effects $\Rightarrow$ selective volatilisation, fractionation
- ✓ Ultraviolet laser: ArF* 193 nm, Nd:YAG 266 nm or 193 nm
  - ✓ Short interaction, minimum thermal effects, minimum fractionation

Applications

Technological samples

- Analysis of technological materials for nuclear power plants
  - Study of corrosion of structural materials for cooling circuits of nuclear reactors by cooling media - molten fluoride salts
  - Study of reaction of CO_2 with Na as nuclear reactor cooling media

CORROSION OF COOLING CIRCUIT STRUCTURAL MATERIALS OF NUCLEAR REACTORS BY COOLING MEDIA - MOLTEN FLUORIDE SALTS

Nuclear power station Temelín Czech Republic

Nuclear power station Dukovany Czech Republic

Molten fluoride salts

Development of new types of reactors:

- **Transmutor** – reactor exploiting a substantial part of the long-term nuclear wastes for transfer into useful power; cooling medium – molten fluoride mixture (LiF-NaF) attacks a surface of piping and heat exchanger parts => corrosion processes study of sample surface by means of LA-ICP-MS
- 3 structural materials for piping and heat exchangers parts are examined:
  - ✓ pure Ni,
  - ✓ Ni-based alloy,
  - ✓ pure Fe with Ni-coating

Molten fluoride salts

1. Ampoules with samples of structural material and salt

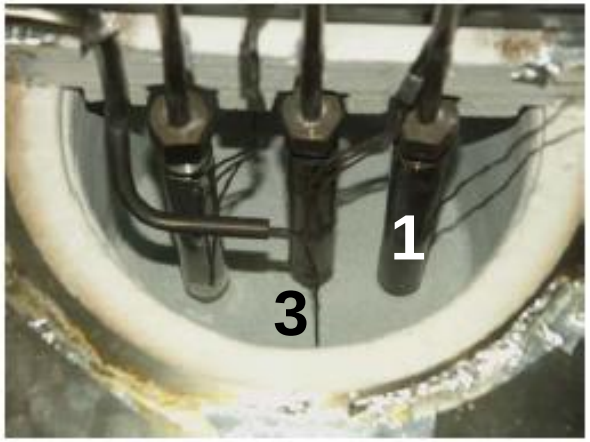

2. Pressure and vacuum system
3. Oven for heating of ampoules
4. Measuring & control system

Molten fluoride salts

Sample is placed into ampoule which is filled with molten fluoride salts for the duration of 112 and 351 hours, respectively

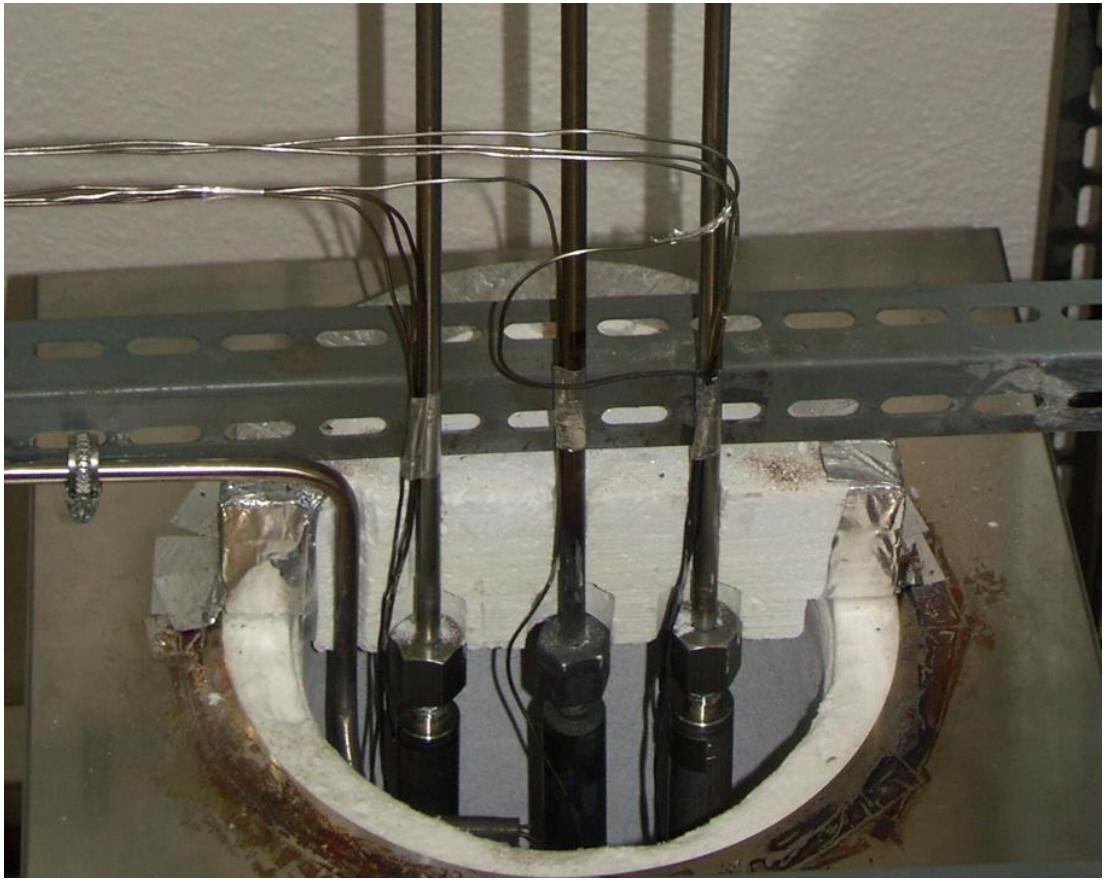

Molten fluoride salts

LA-ICP-MS experiments:
laser wavelength – 213 nm, laser spot size – 6 μm, repetition rate 20 Hz, laser power energy density 14 J cm^{-2}, scan rate 6 μm s^{-1}
Steep increase of Ni signal means the start of sample surface and drop of Na signal to background value means end of affected zone. Difference between these two values give a thickness of affected zone. Start of sample surface is marked as „0“.

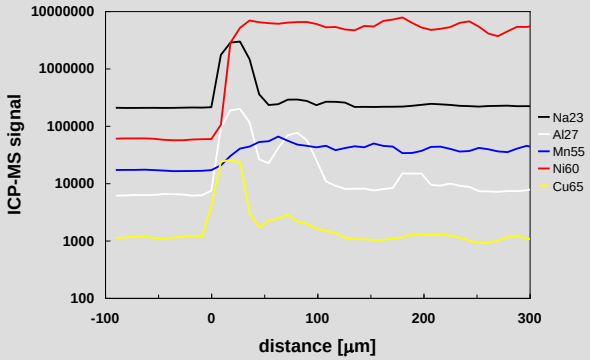

pure Ni

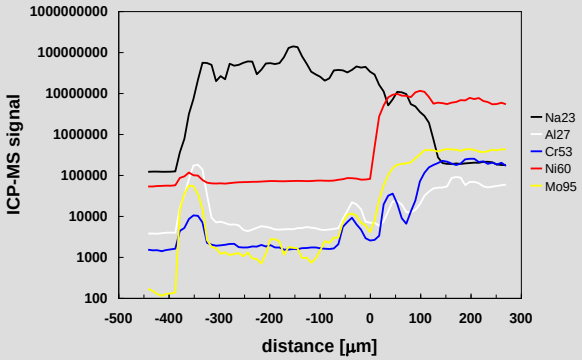

Ni-based alloy

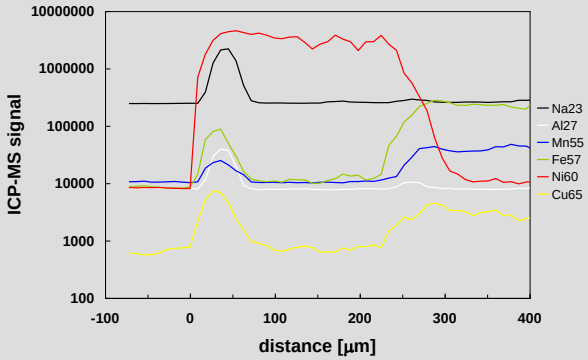

pure Fe with Ni-coating

Sample	Ni201 112 h	Ni201 351 h	A071EV 112 h	A071EV 351 h	Ni-coating 112 h	Ni-coating 351 h
Thickness [μm]	54	63	144	162	63	81

2D maps of corrosion of surface – testingf ampoules

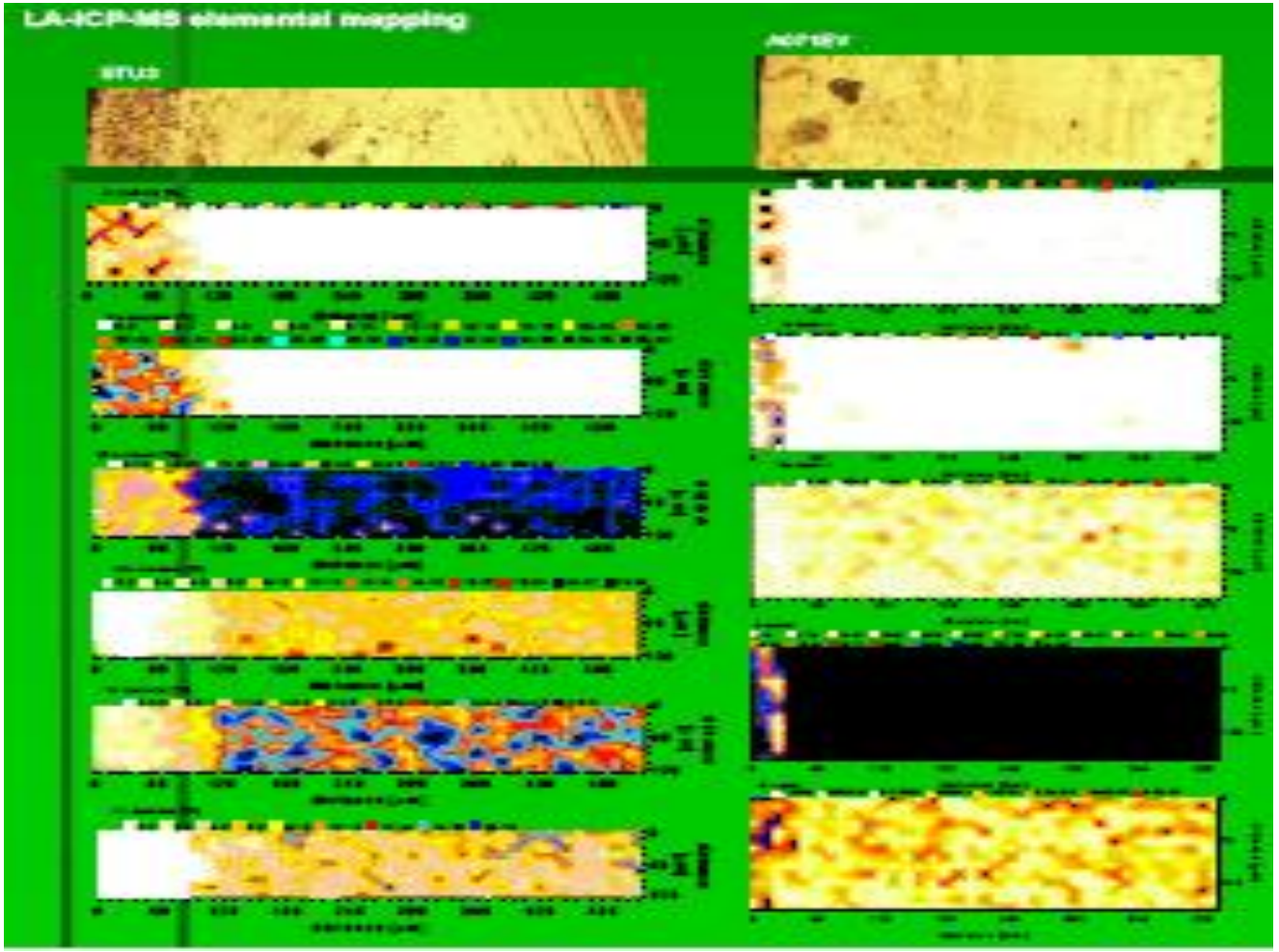

REACTION OF CO_2 WITH SODIUM - NUCLEAR REACTOR COOLING MEDIA

- **Sodium-cooled fast reactor (SFR)** – Generation IV of nuclear reactors; cooling medium – liquid sodium; heat is transferred from sodium circuit in heat exchanger to CO_2 . Possible reaction of sodium with CO_2 at elevated temperatures is experimentally studied => determination of carbon in sodium by means of LA-ICP-OES and ICP-OES

T. Vaculovič*, V. Kanický, O.Matal

Molten Na-CO_2 interaction

A new apparatus was designed for sodium melting under CO_2 atmosphere at high temperature.
Apparatus is placed into glove box with CO_2 atmosphere.
Furnace is heated up to 300, 350 and 450 °C, respectively.
180 minutes of melting + 120 min cooling down

Two ways of carbon content determination

1. Laser ablation of solidified sodium with ICP-OES detection (calibration pellets with two types of matrix – NaCl and $Na_2B_4O_7$*10 H_2O)
2. Dissolution of solidified sodium with water vapor – nebulization into ICP-OES (calibration solution with NaCl, $NaNO_3$ and NaOH matrices)

Molten Na-CO_2 interaction

ICP-OES experiments

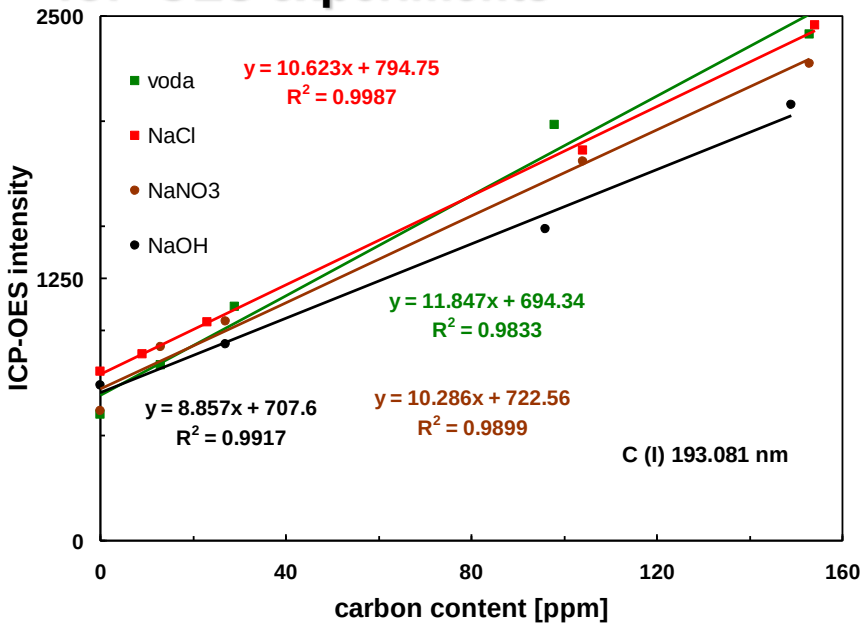

LA-ICP-OES experiments

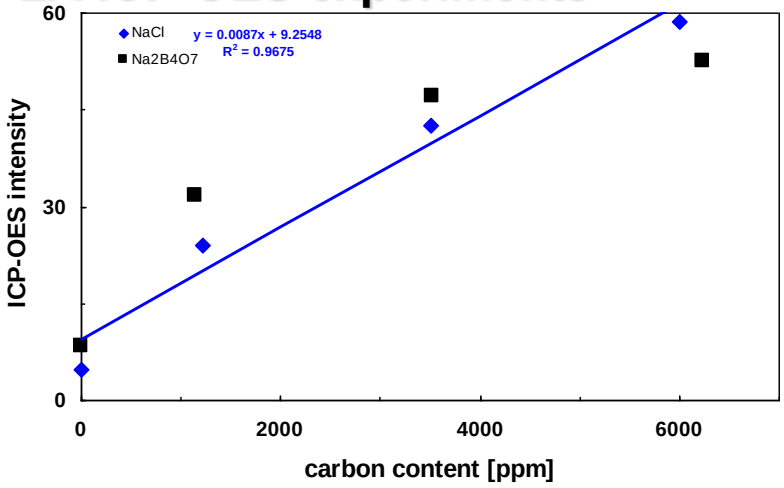

matrix	matrix effect (I_{matrix}/I_{water}*100)	
	C (I) 193 nm	C (I) 247 nm
NaCl	89	89
$NaNO_3$	87	91
NaOH	74	77

	carbon content [µg g^{-1}]	
	LA-ICP-OES	ICP-OES
Non-melted Na	< LOD (ca 500)	< LOD (ca 300)
Na melted at 300°C	3700	4050
Na melted at 350°C	2000	3100
Na melted at 450°C	< LOD	-[1]

[1] – not measured

Geology

- 2D-mapping of granite by LIBS and LA-ICP-MS

Exploratory study - granite

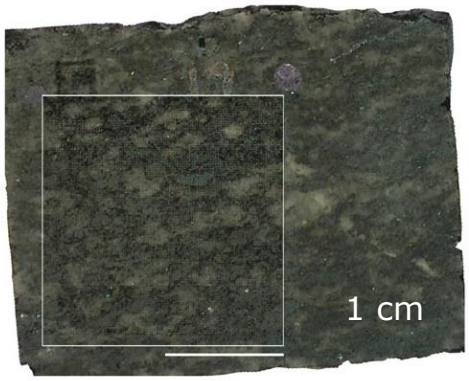

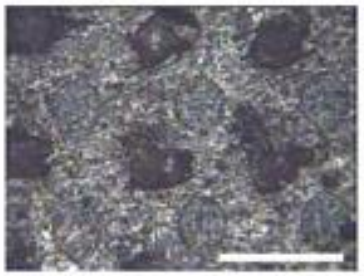

200 µm

LIBS
120 µm laser spot diameter, 2 laser pulses per sample point

LA-ICP-MS
hole drilling mode, 110 µm laser spot diameter, 20 laser pulses per sample point, distance between individual laser spots was 200 µm

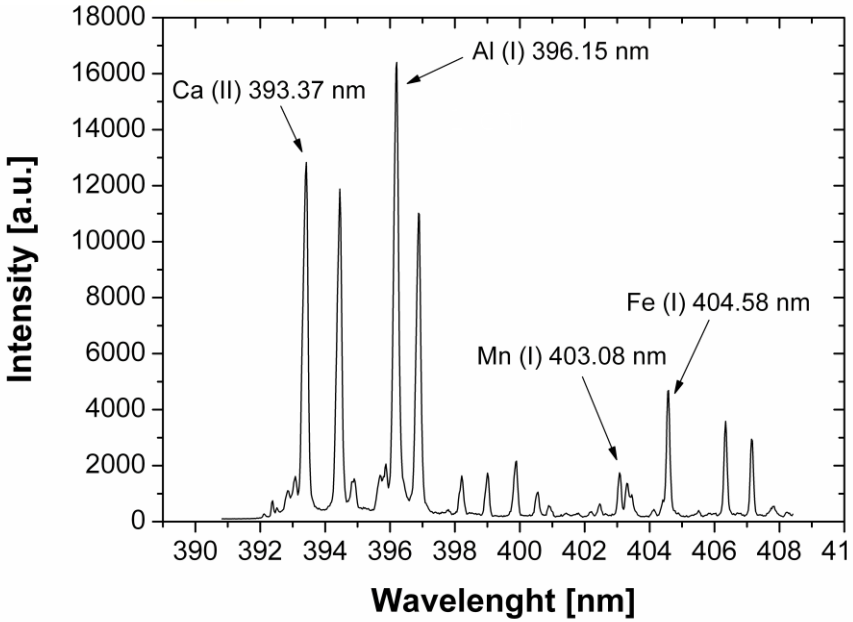

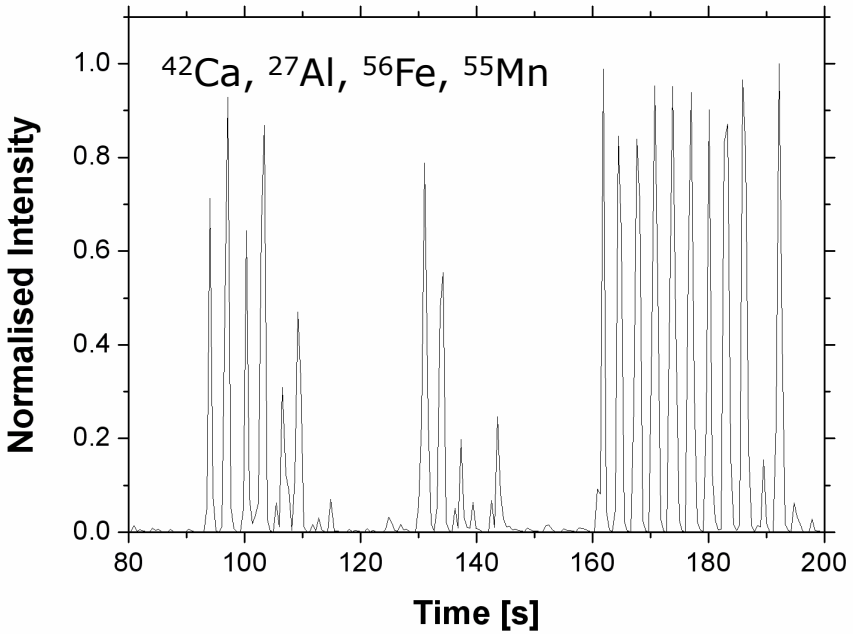

K. Novotný, J. Kaiser, M. Galiová, et al.: Mapping of different structures on large area of granite sample using laser-ablation based analytical techniques, an exploratory study, Spectrochimica Acta Part B 63 (2008) 1139–1144.

K. Novotný, J. Kaiser, M. Galiová, et al.: Mapping of different structures on large area of granite sample using laser-ablation based analytical techniques, an exploratory study, Spectrochimica Acta Part B 63 (2008) 1139–1144.

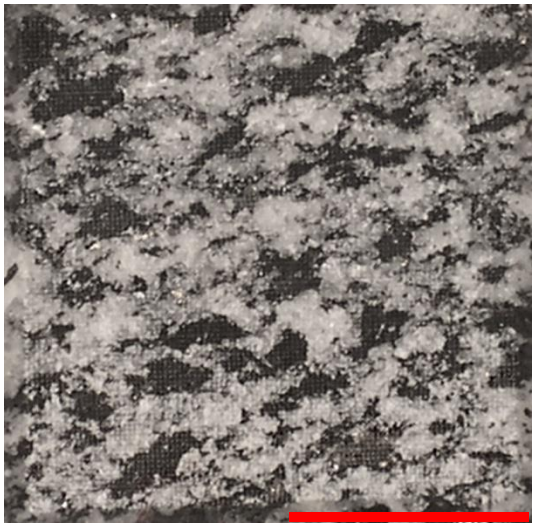

photo

1 cm

Ca

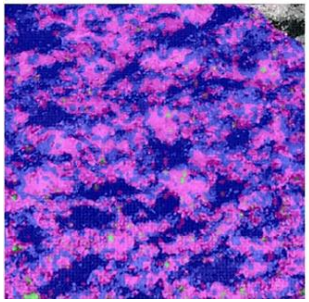

Fe

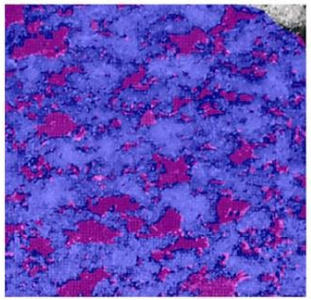

maps

LIBS

LA-ICP-MS

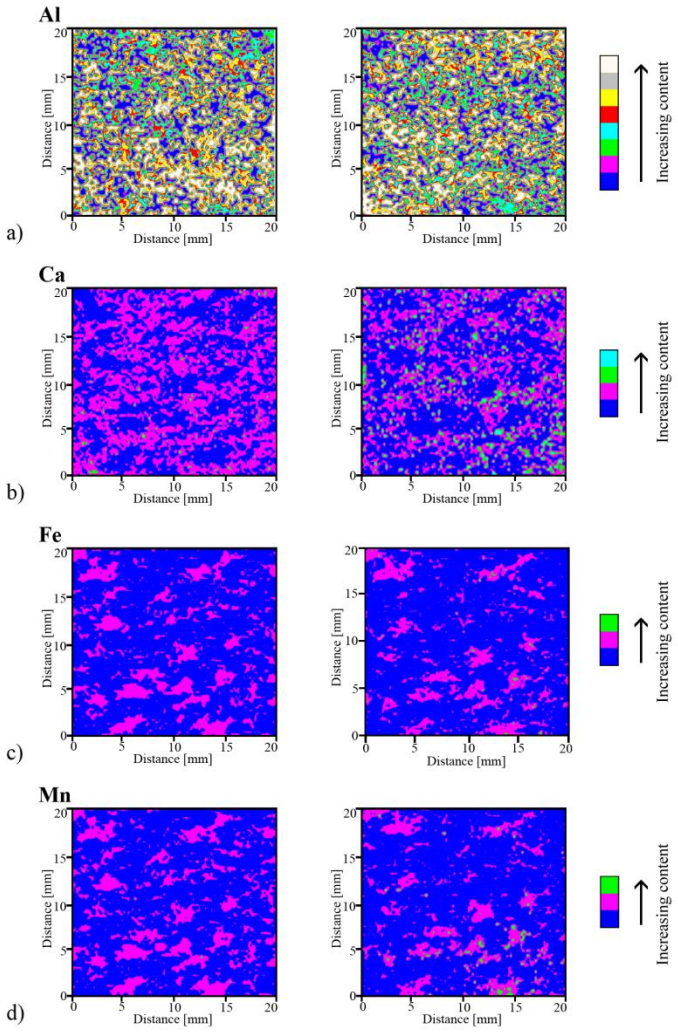

Archaeology

- Fossile bones
- Animal tooth

BONES ELEMENTAL MAPPING BY LA-ICP-MS AND DOUBLE PULSE LIBS

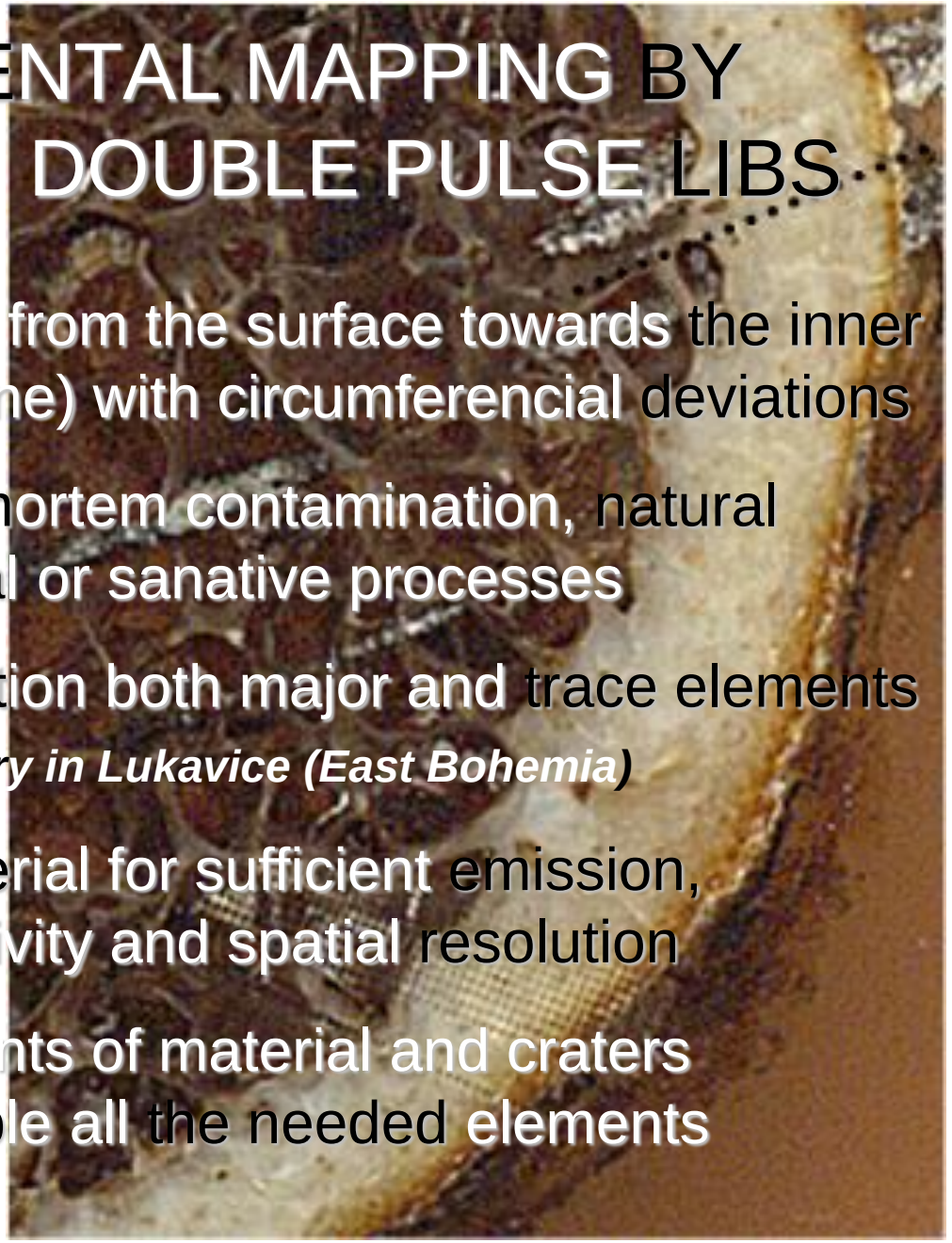

- Radial gradient in direction from the surface towards the inner part of compacta (dense bone) with circumferencial deviations
- Resolution among a post-mortem contamination, natural metabolism and pathological or sanative processes
- Local analysis – determination both major and trace elements

LIBS? ***Luetic Tibia from ossuary in Lukavice (East Bohemia)***

- single pulse – a lot of material for sufficient emission, large craters => poor sensitivity and spatial resolution
- double pulse – small amounts of material and craters similar to LA-ICP-MS – visible all the needed elements

LA-ICP-MS

Spacing: 0.15 mm, 10 × 30 craters: 0.1 mm in diameter

Orthogonal double pulse LIBS

Spacing: 0.25 mm, line scan 17 craters: 0.2 mm in diameter

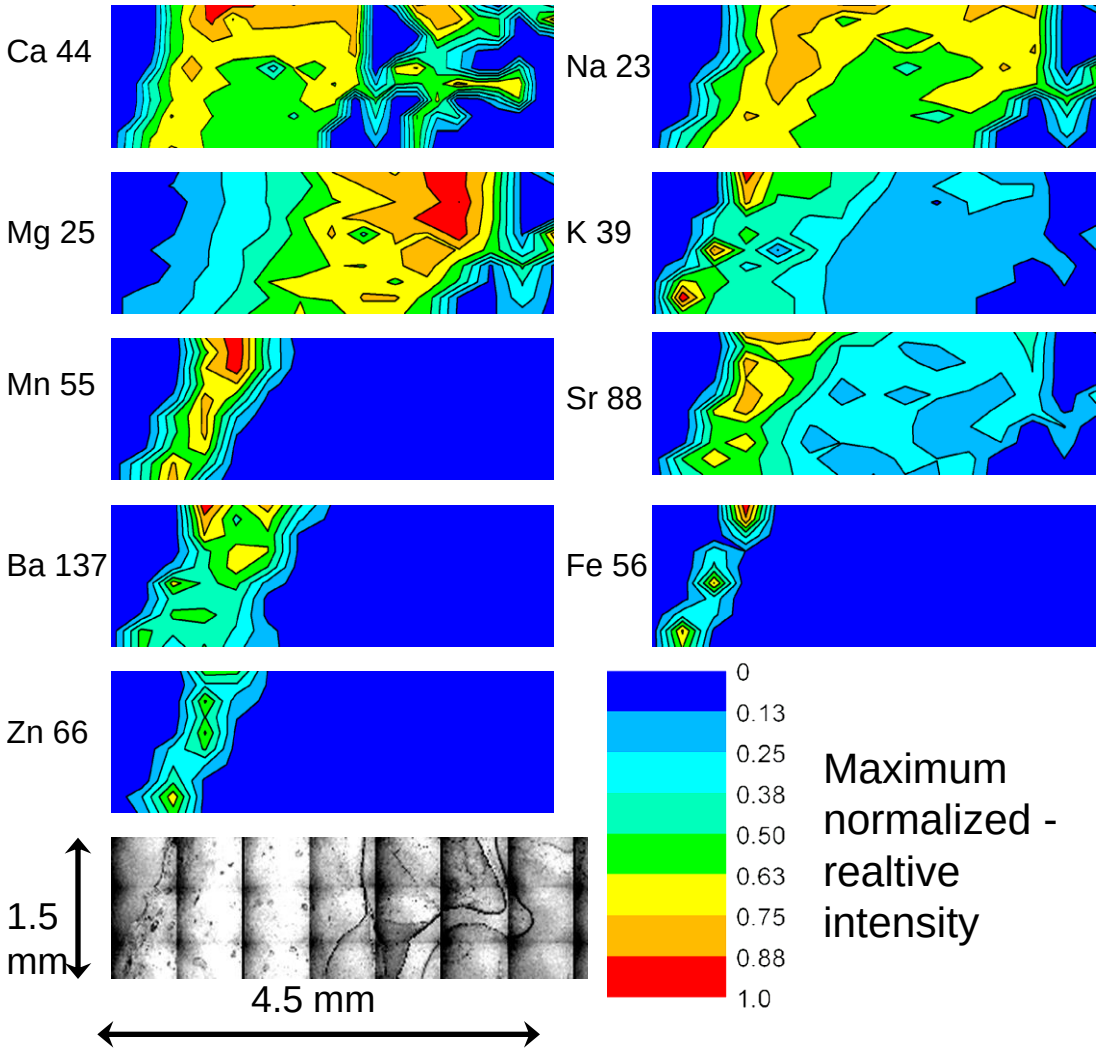

Maximum normalized - realtive intensity

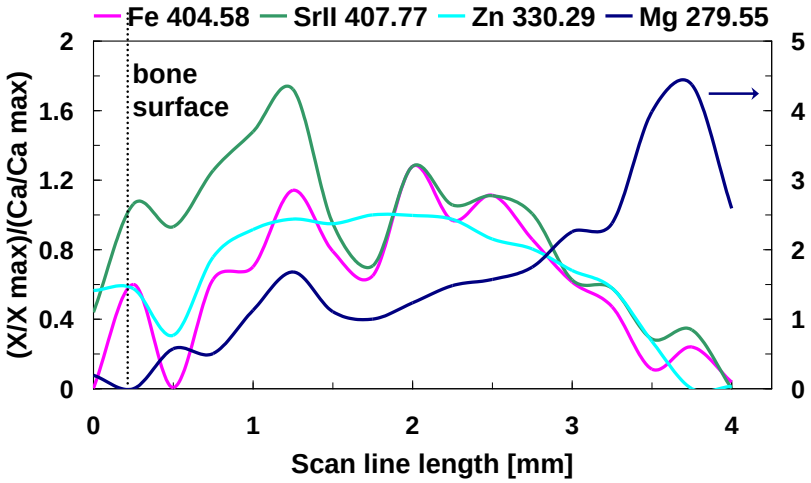

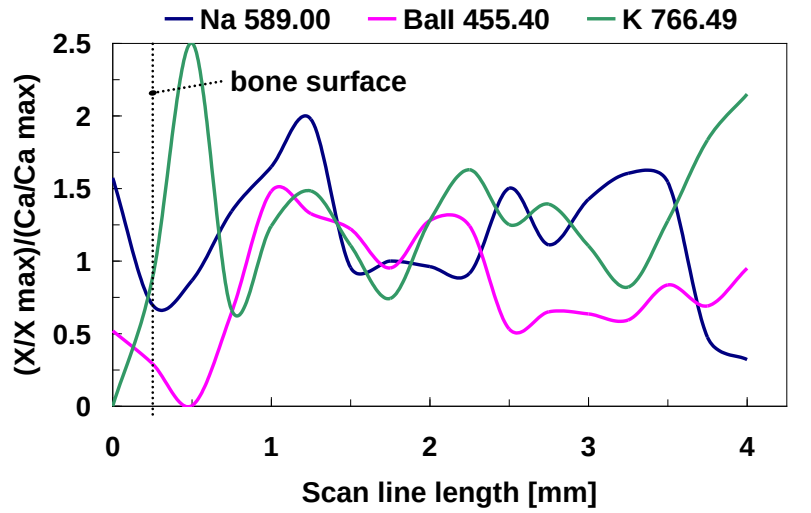

Ca – normalized intensities

Bone mapping results

- **Ca, Na** and **P** are homogenously distributed in the sample.
- **Mg** relative depletion in external part of the bone.
- **Zn** is accumulated in external part of the compact bone, this observation is in accordance with results of other studies. This accumulation of Zn is due to bone resorption and osteogenesis, pathological evolutions or, due to post-mortem alterations too. In this case, correspondence with pathological process is most probable.
- **Pb, Ba** are accumulated in external part of the compact bone, similarly as zinc; Lead accumulation is due to diagenesis.
- **Sr** is only slightly accumulated in periosteal region of bone or homogenously distributed.
- Analogies in strontium, barium and lead distributions are due to their similar metabolism

Bear´s tooth

The photographs of the studied sample. The investigated tooth was excavated at Dolní Věstonice II-Western Slope, South Moravia, Czech Republic (archaeological research in 1987) and was situated closely to the famous Upper Palaeolithic triple-burial of young people. This locality is dated to 26 640 ± 110 BP (uncalibrated ^{14}C data) and belongs to Gravettian. On the left image the investigated cross section of the analysed tooth (canin-C_1) that belongs to brown bear (*Ursus arctos*) is shown (red box). Increments of cementum of teeth´s root were studied in according to determine the seasonality. This bear died at the age of 14 years in between summer and autumn season (August to October). The bars have a length of 1 cm.

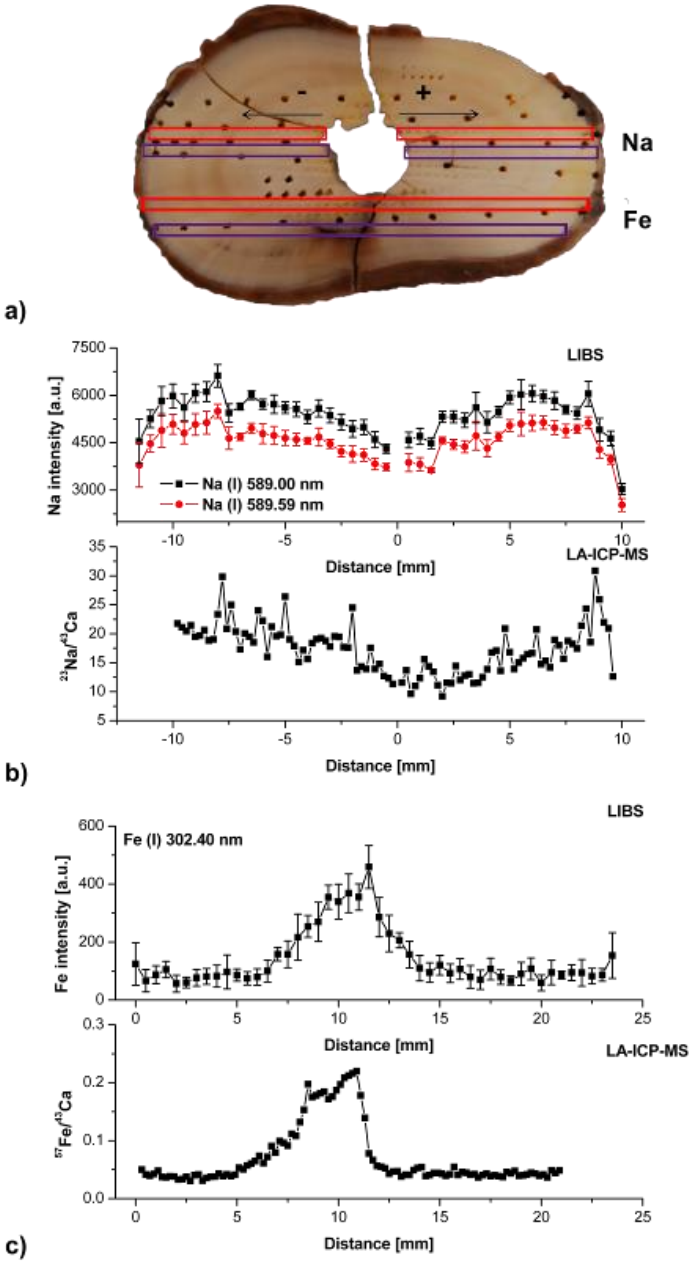

Comparison of the elemental distribution of b) Na and c) Fe obtained on the cross-sections of fossil brown bear (*Ursus arctos*) canine tooth dentine utilizing LIBS and LA-ICP-MS. The LIBS and LA-ICP-MS line scans were positioned to the places shown on the photograph a).

M. Galiová, J. Kaiser, F. J. Fortes, K. Novotný, R. Malina, L. Prokeš, A. Hrdlička, T. Vaculovič, M. Nývltová Fišáková , J.Svoboda, J. J. Laserna: Multielemental analysis of prehistoric animal teeth by laser-induced breakdown spectroscopy and Laser Ablation Inductively Coupled Plasma Mass Spectrometry, zasláno do JASSu, 2009

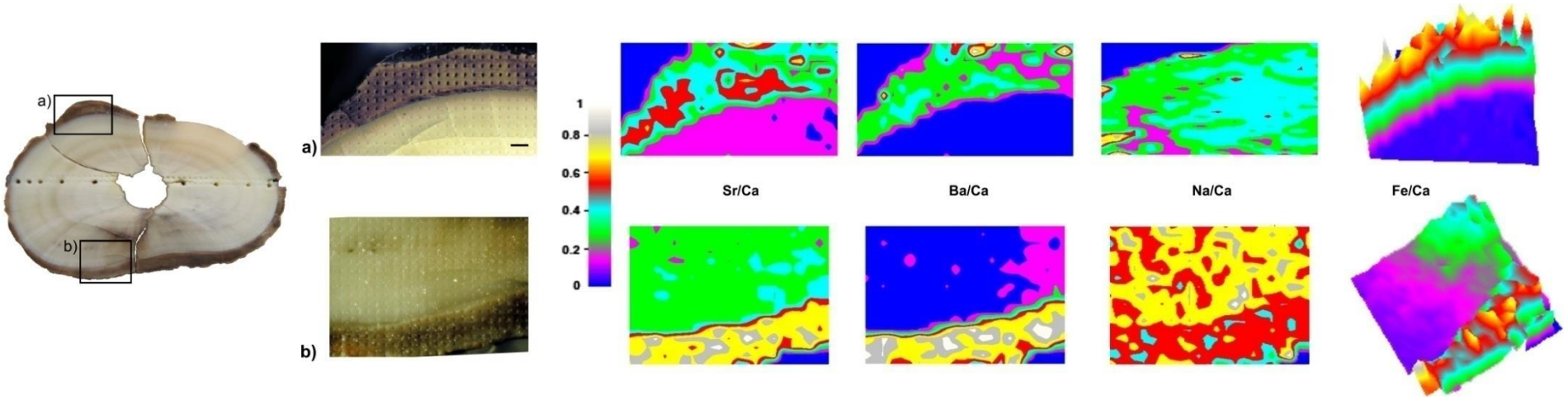

The results of LA-ICP-MS elemental mapping in two different areas (a), b)) of the sample. The bar has a length of 400 μm.

M. Galiová, J. Kaiser, F. J. Fortes, K. Novotný, R. Malina, L. Prokeš, A. Hrdlička, T. Vaculovič, M. Nývltová Fišáková , J.Svoboda, J. J. Laserna:
Multielemental analysis of prehistoric animal teeth by laser-induced breakdown spectroscopy and Laser Ablation Inductively Coupled Plasma Mass Spectrometry, submitted JASS, 2009

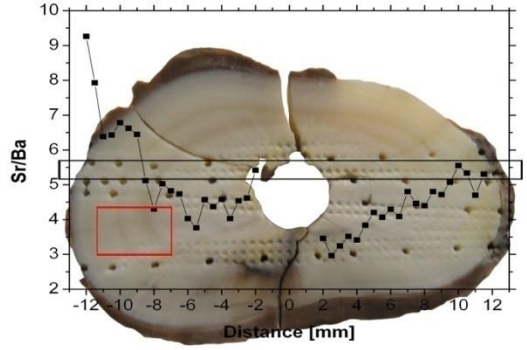

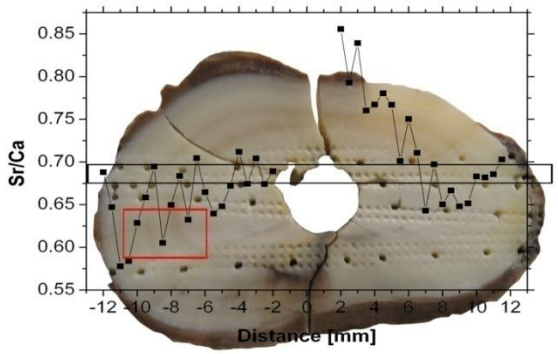

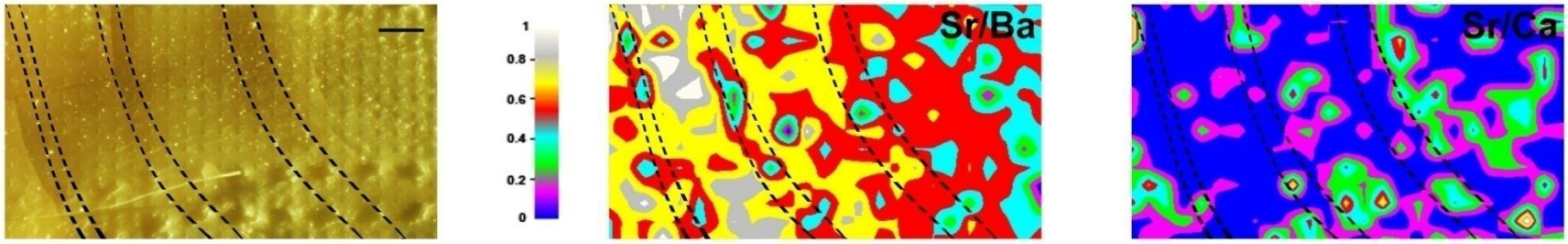

The Sr/Ca and Sr/Ba ratios derived from LIBS line scan and LA-ICP-MS mapping. With dotted lines the different regions on the teeth cross section are shown. The bar has a length of 500 μm.

M. Galiová, J. Kaiser, F. J. Fortes, K. Novotný, R. Malina, L. Prokeš, A. Hrdlička, T. Vaculovič, M. Nývltová Fišáková , J.Svoboda, J. J. Laserna:
Multielemental analysis of prehistoric animal teeth by laser-induced breakdown spectroscopy and Laser Ablation Inductively Coupled Plasma Mass Spectrometry, submitted toJASS, 2009

a) estimation of the sample hardness via magnesium ionic to atomic line intensity ratios. The estimated hardness characteristic was proved by microhardness measurements b). The ablation crater depths calculated from the cross sections measured by an optical profilometer are shown for comparison on c).

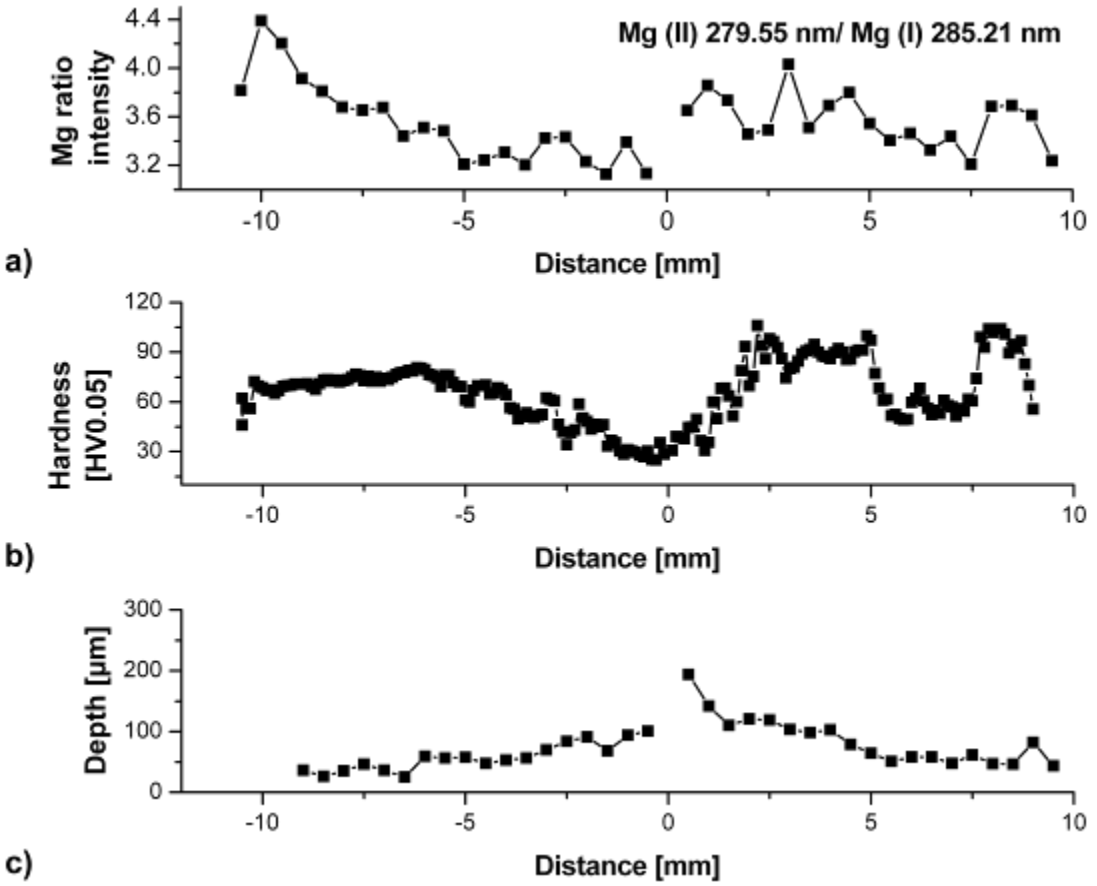

M. Galiová, J. Kaiser, F. J. Fortes, K. Novotný, R. Malina, L. Prokeš, A. Hrdlička, T. Vaculovič, M. Nývltová Fišáková , J.Svoboda, J. J. Laserna:
Multielemental analysis of prehistoric animal teeth by laser-induced breakdown spectroscopy and Laser Ablation Inductively Coupled Plasma Mass Spectrometry, submitted to JASS, 2009

49

root

Sr

2,5*1,5cm

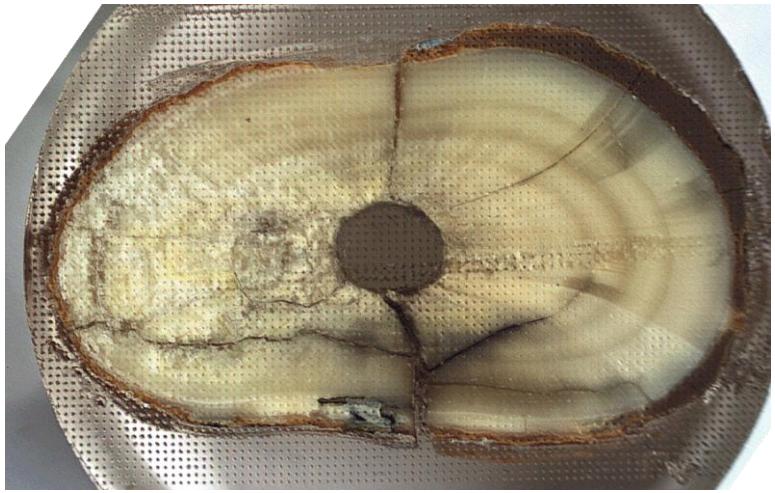

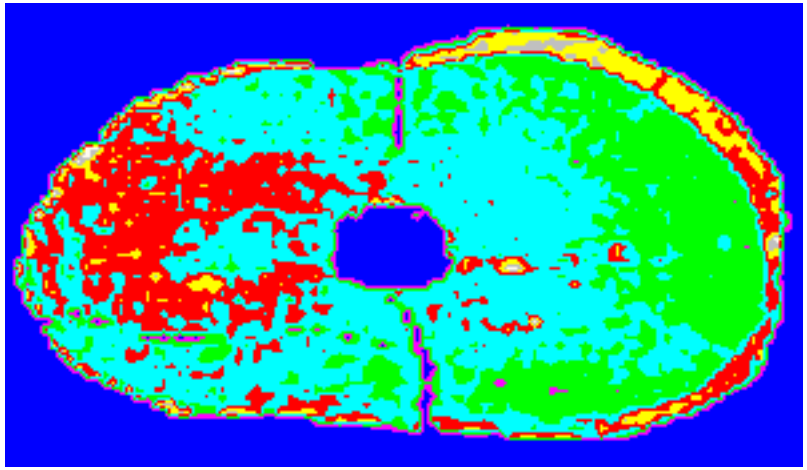

crown

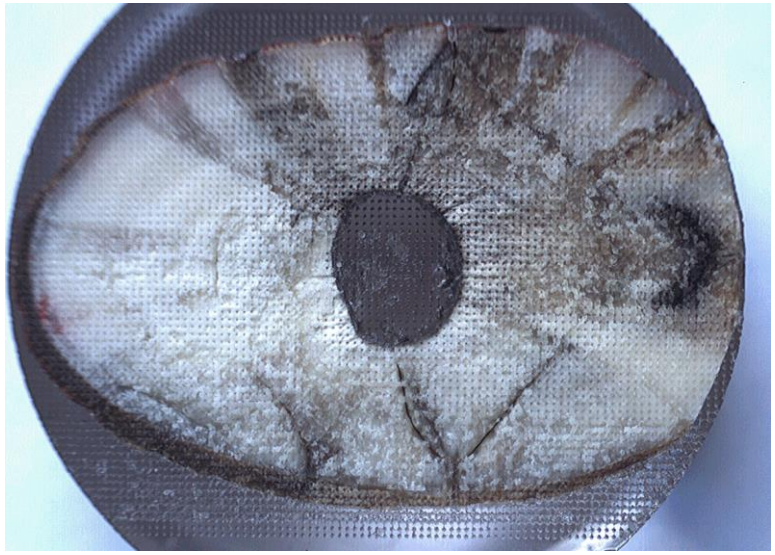

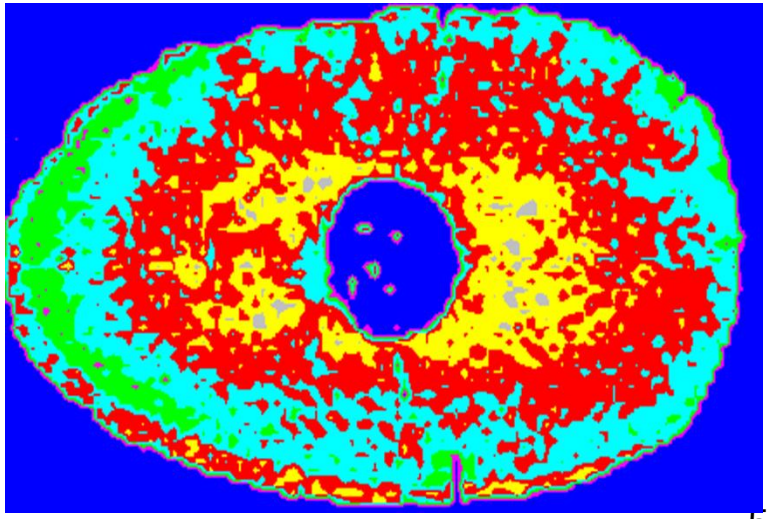

50

Environmental

- Uroliths – renal calculi
- Fish scales

UROLITH LOCAL ANALYSIS

Kidney stones, urinary stones (**renal calculi, urolithiasis) =** solid concretions (crystal aggregations) of dissolved minerals in urine calculi typically form inside kidneys, ureter, urethra, bladder, prostate

To date over 200 components have been found in calculi; however, the most common constituents of kidney stones are:

- Calcium Oxalate Monohydrate (**Whewellite**); $CaC_2O4 \cdot H_2O$
- Calcium Oxalate Dihydrate (**Weddellite**); $CaC_2O4 \cdot 2H_2O$
- Magnesium Ammonium Phosphate Hexahydr. (**Struvite**); $MgNH_4PO_4 \cdot 2H_2O$
- Ca Phosphate &Carbonate (**Carbonate Apatite**); $Ca_{10}(PO_4 \cdot CO_3OH)_6(OH)_2$
- Calcium Phosphate, Hydroxyl Form (**Hydroxyl Apatite**); $Ca_{10}(PO_4)_6(OH)_2$
- Calcium Hydrogen Phosphate Dihydrate (**Brushite**); CaHPO4 · 2H2O
- Uric Acid; $C_5H_4N_4O_3$
- Cystine; $(SCH_2CH(NH_2) \cdot COOH)_2$
- Sodium Acid Urate; $C_5H_3N_4O_3Na \cdot H_2O$
- Tricalcium Phosphate (**Whitlockite**); $Ca_3(PO4)_2$
- Ammonium Acid Urate; $NH4H \cdot C_5H_2O_3N_4 \cdot H_2O$
- Magnesium Hydrogen Phosphate Trihydrate (**Newberyite**); $MgHPO_4 \cdot 3H_2O$

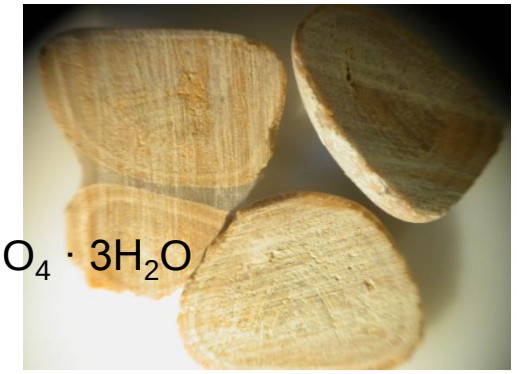

Layered structure: growth of uroliths

Designed procedure

1. **Average elemental contents in uroliths** by PN-ICP-MS after acid mixture decomposition
2. **LA-ICP-MS calibration** with homogenized **urolith pellets** and assignment of content values found using PN-ICP-MS to the pellets.
3. **LA-ICP-MS calibration** with pressed pellet of powdered **SRM NIST 1486 Bone Meal.**

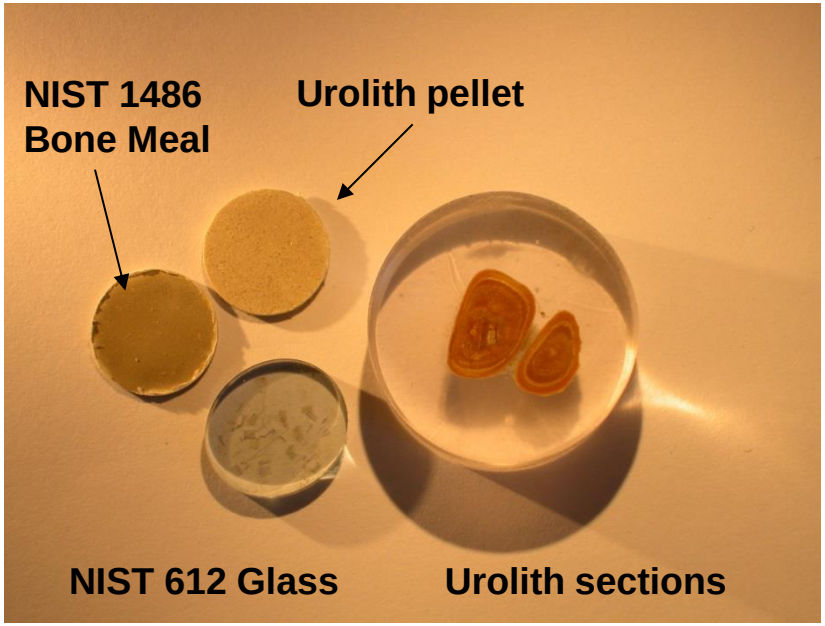

4. **LA-ICP-MS elemental distribution recording** = line of single-spot ablation events directed perpendicularly to layered structure of urolith section
5. **LA-ICP-MS calibration using:**
   - NIST 1486 Bone Meal
   - urolith pellets with contents by PN-ICP-MS
   - NIST 612 Glass
6. **Calculation of concentration profile of uroliths**

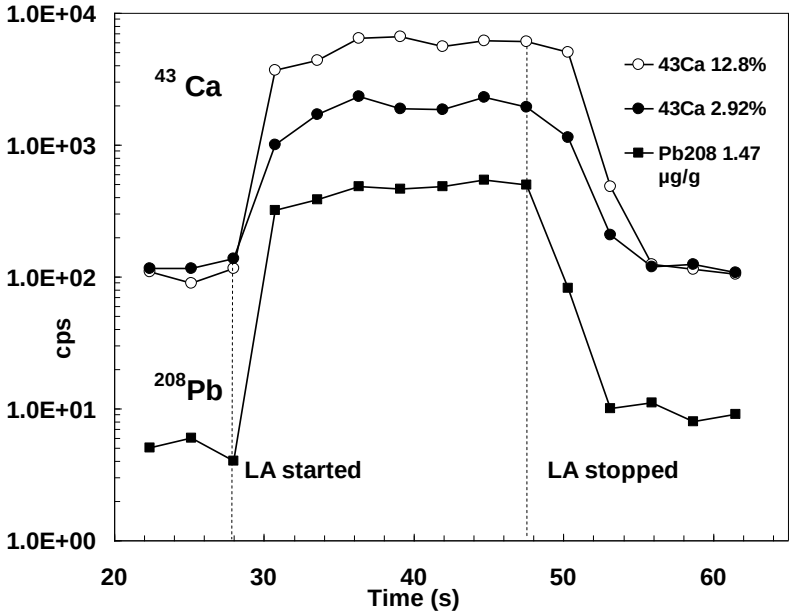

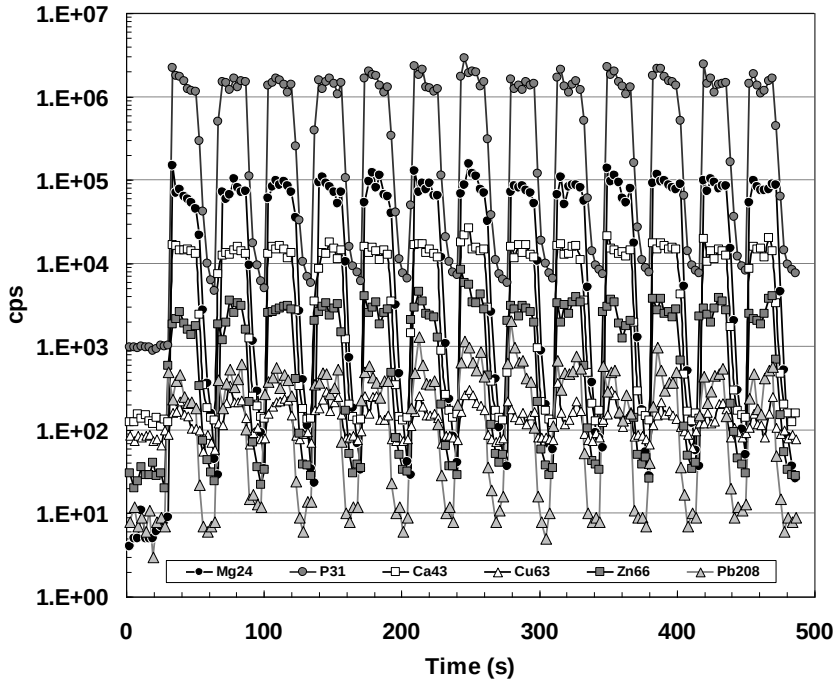

- Lines of single spots
- Laser spot size 55 µm
- Crater distance 110 µm

- Repetition rate 20 Hz
- Fluence of 3 J cm^{-2}
- No internal standard ICP-MS

Calibration Zn, Pb, Cu powdered urolith pressed pellets

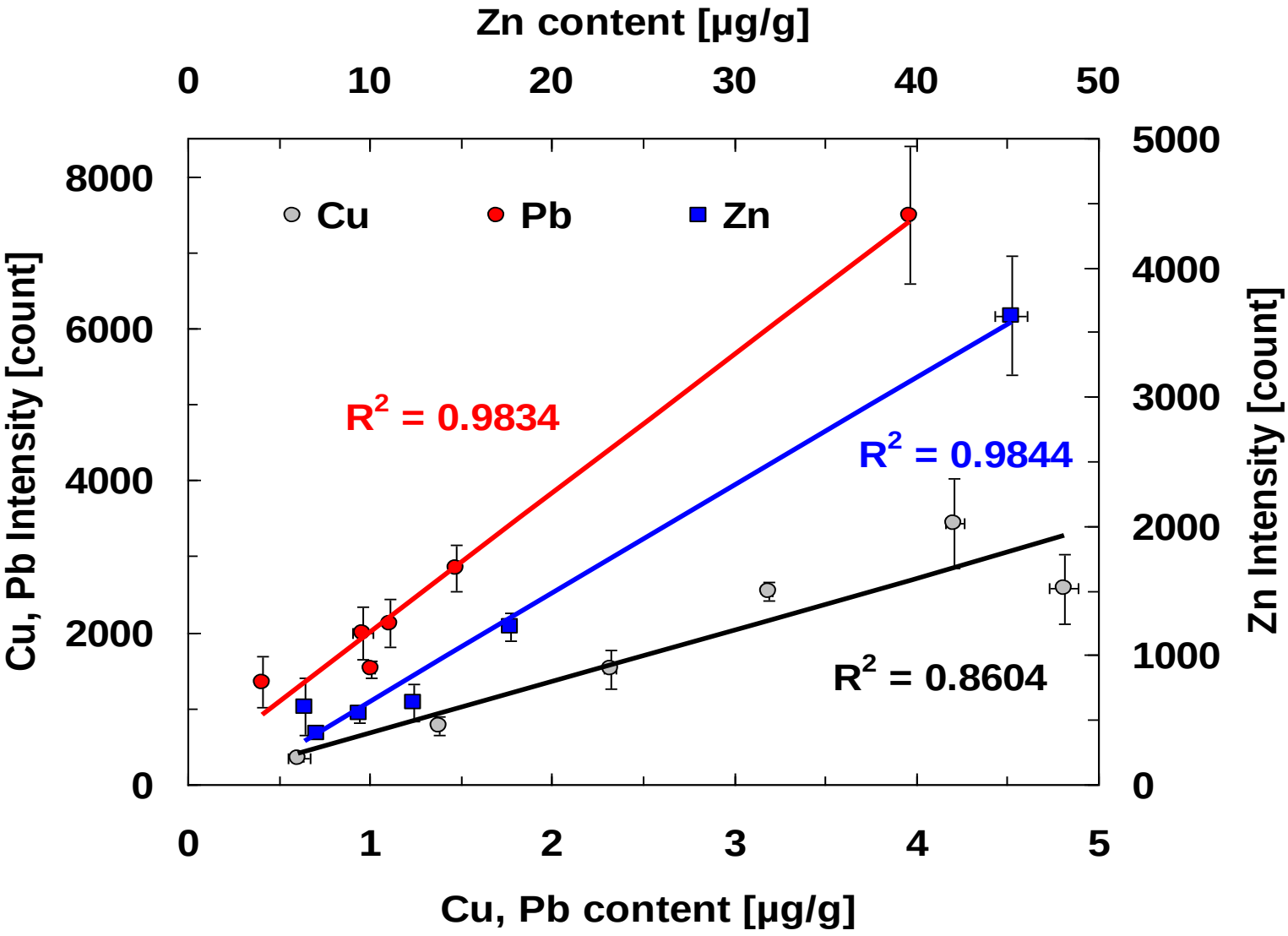

Calibration Ca, P: powdered urolith pressed pellets

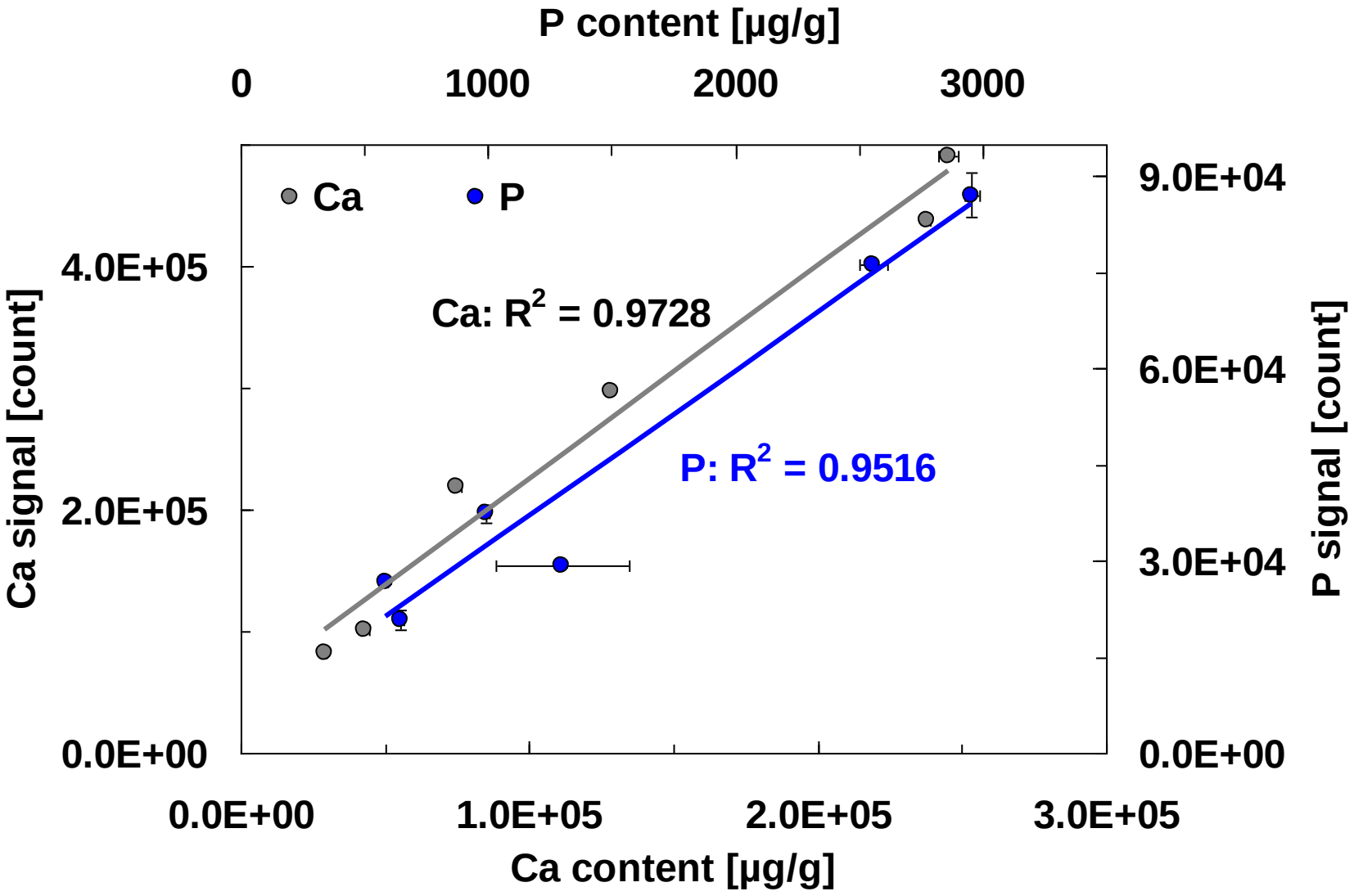

Radial profile of urolith - signal

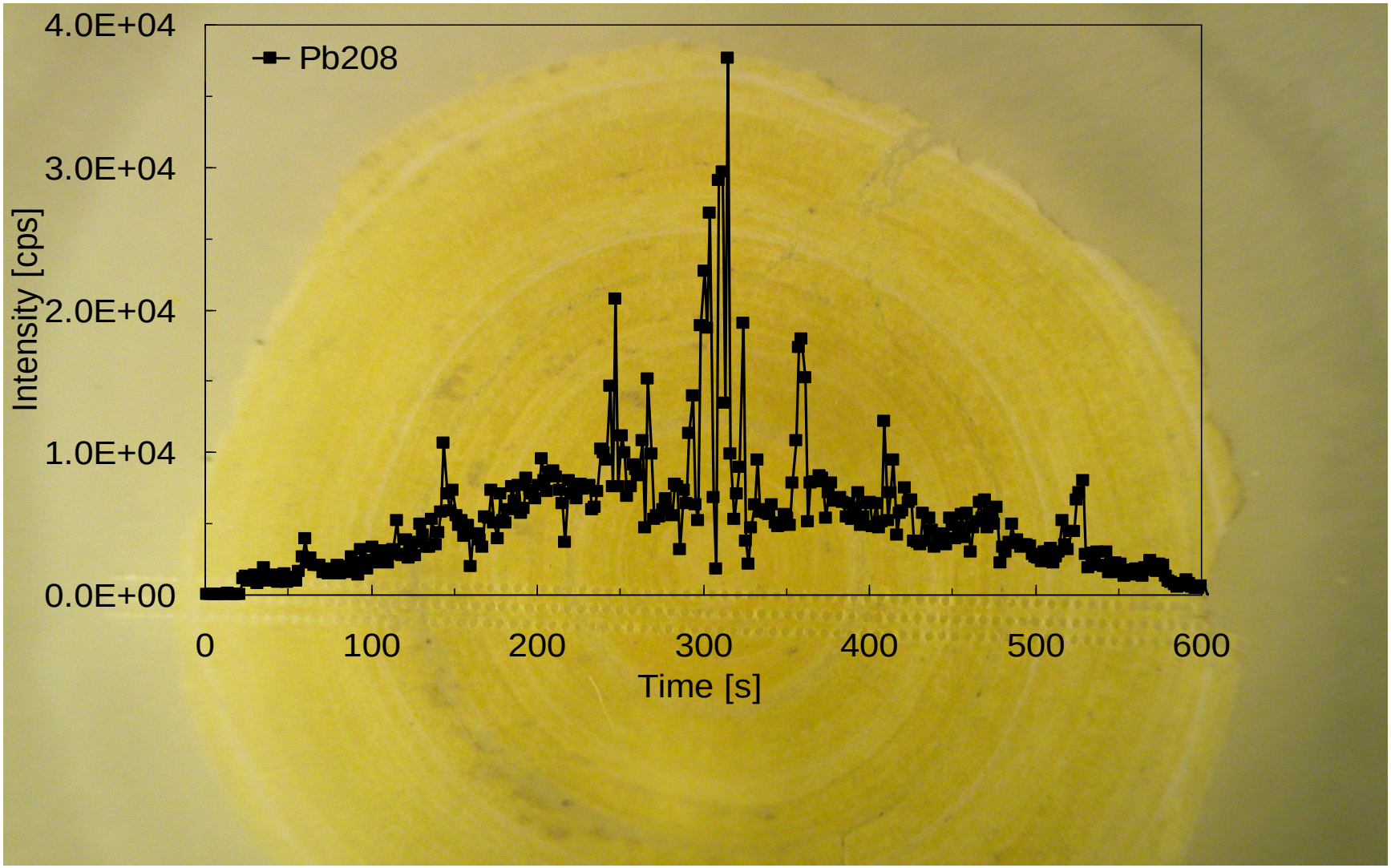

Urolith section, complementarity of apatite and oxalate vs urate, quatification – pressed pellets

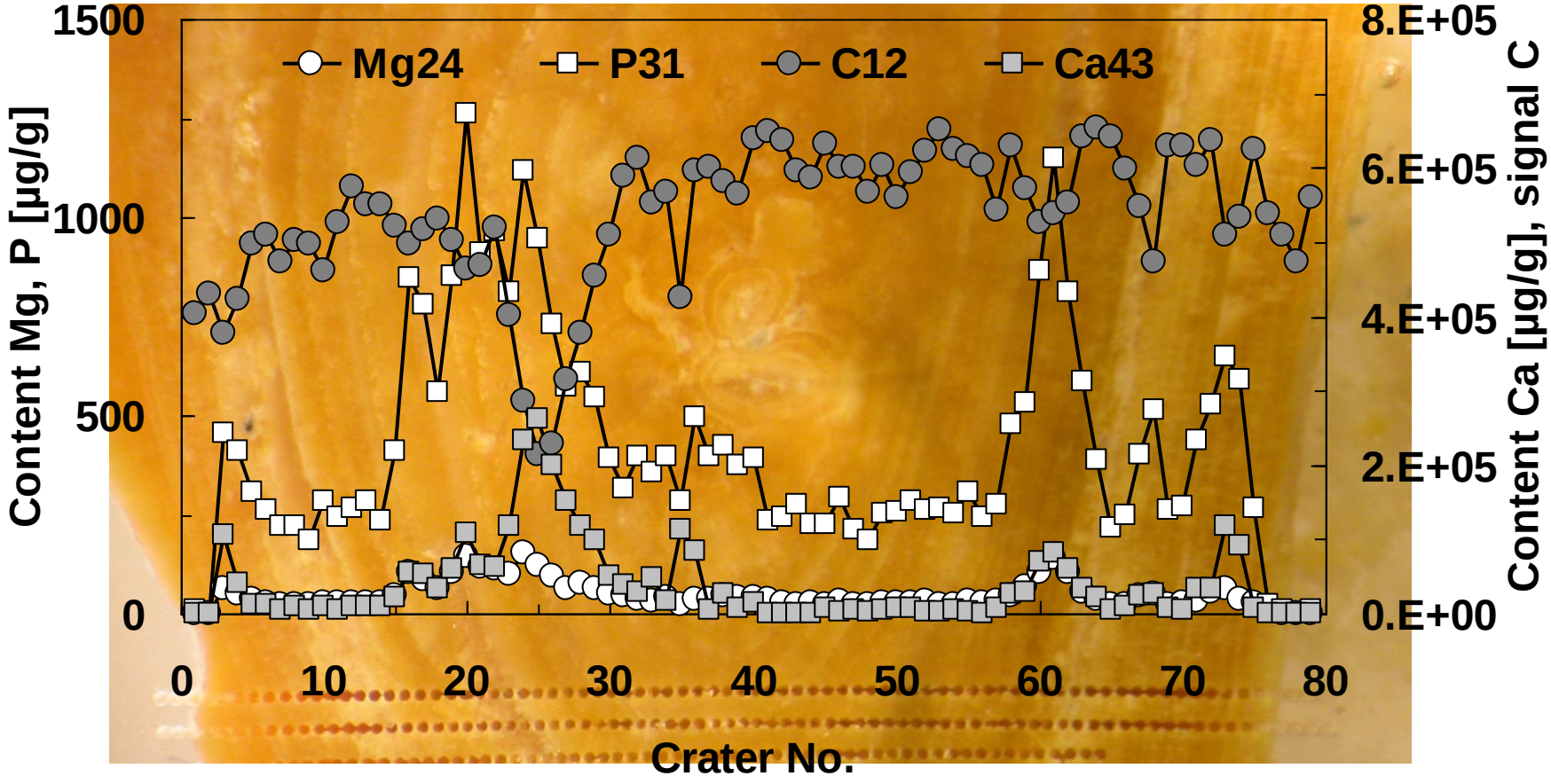

V Konecna, M. Novackova, M. Hola, P. Martinec, J. Machat, V. Kanicky

2D graph of distribution of Ca concentration in sample 10806

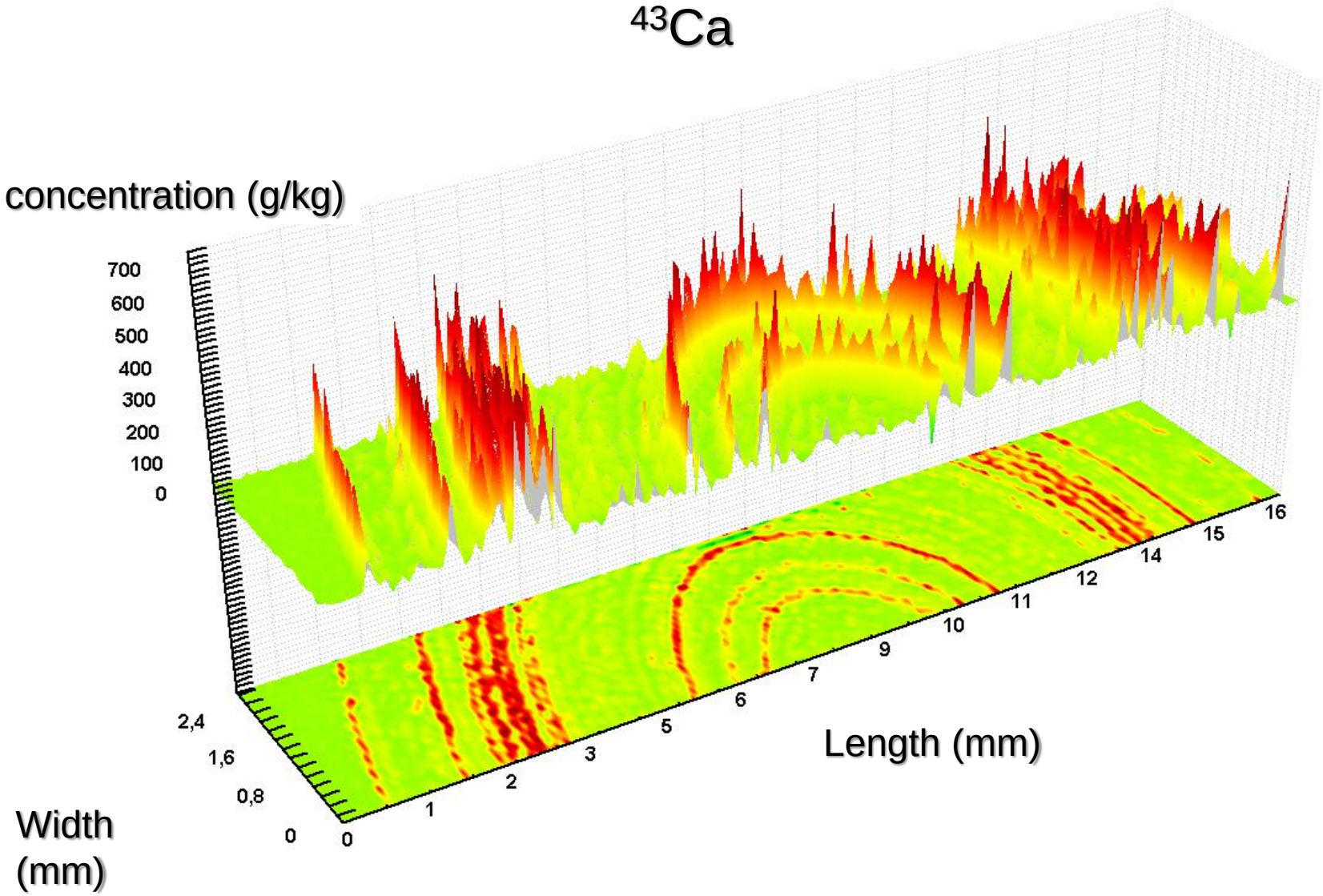

2D graph of distribution of P concentration in sample 10806

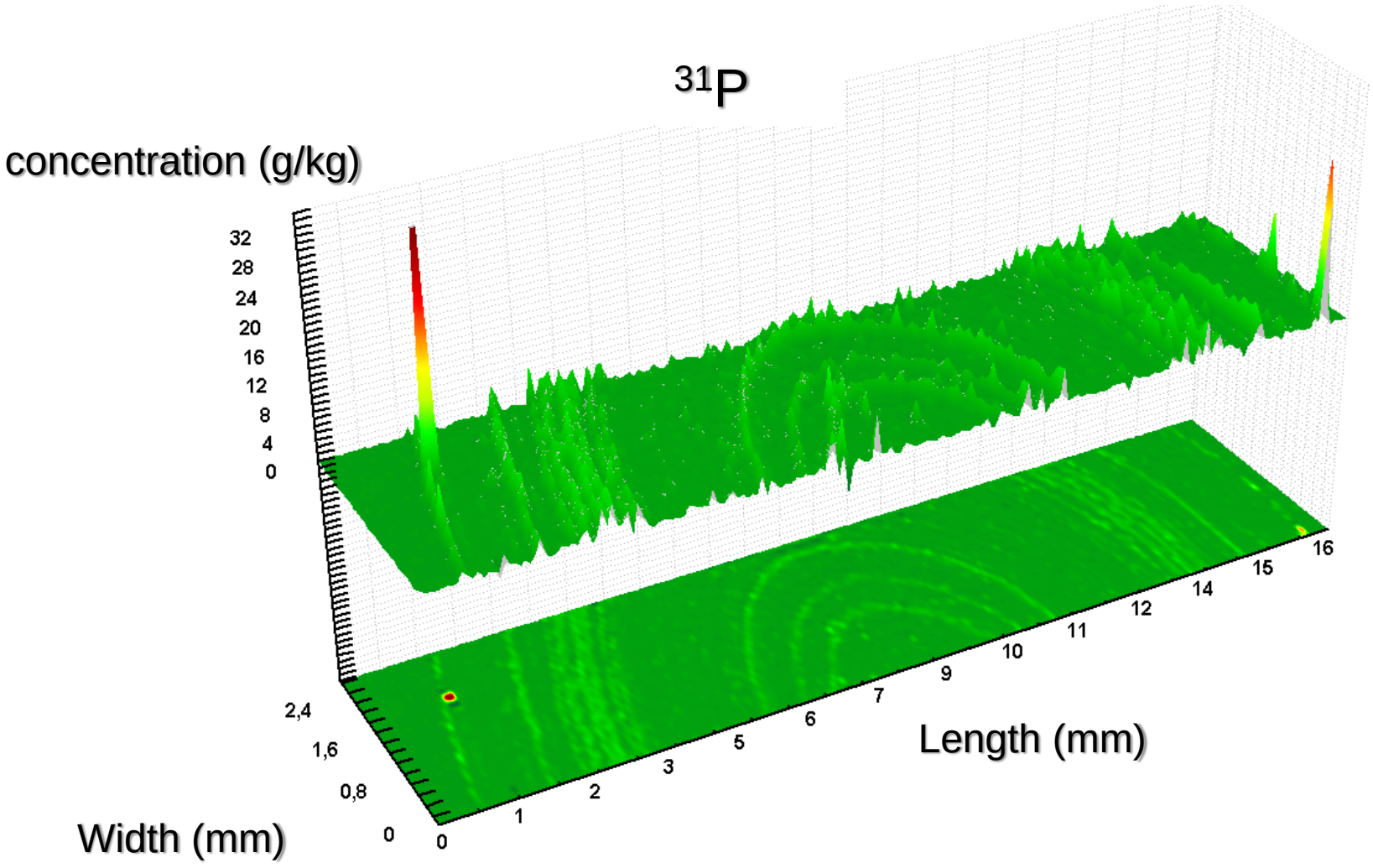

2D graph of distribution of Mg concentration in sample 10806

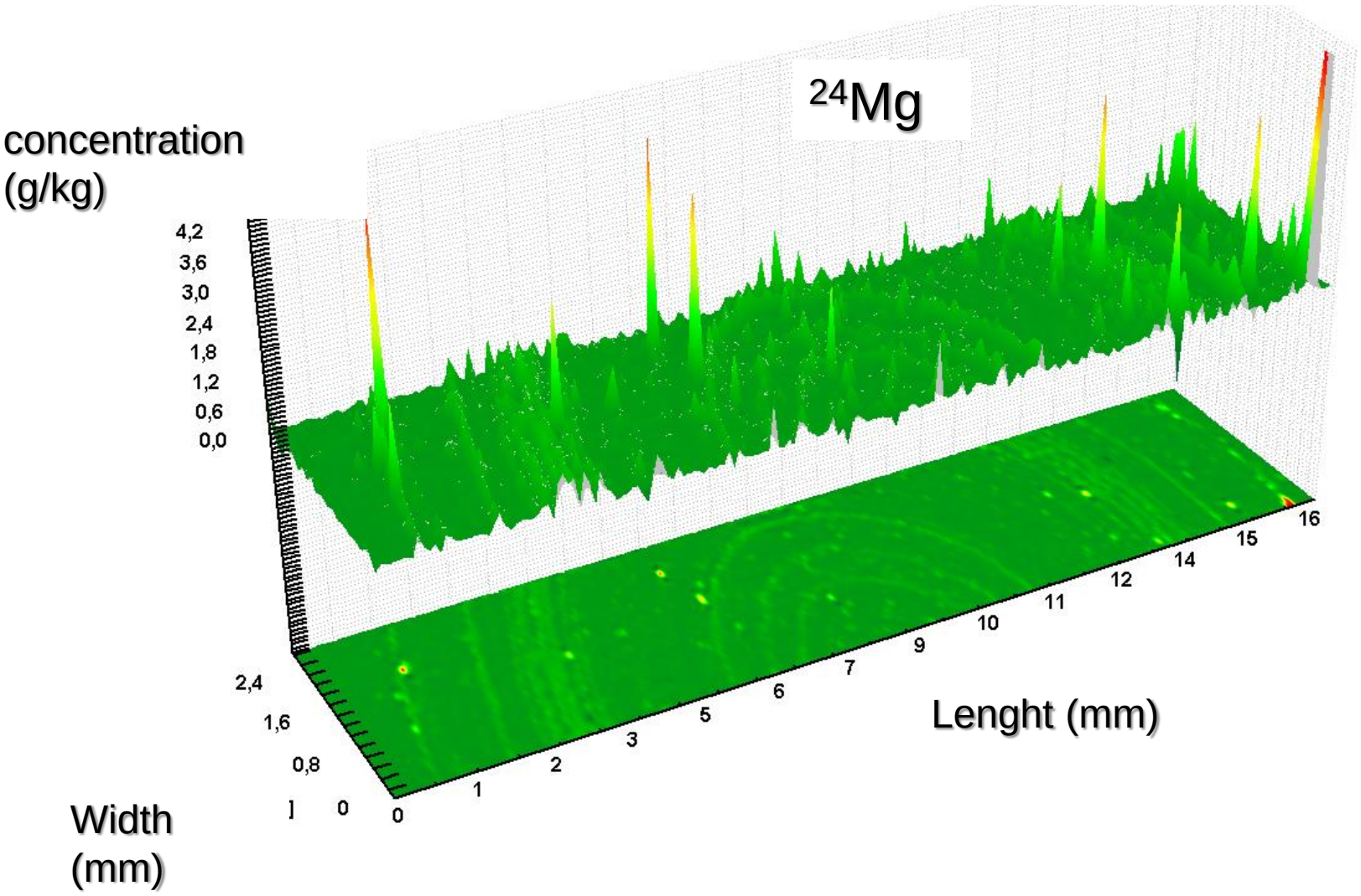

2D graph of distribution of C presence in sample 10806

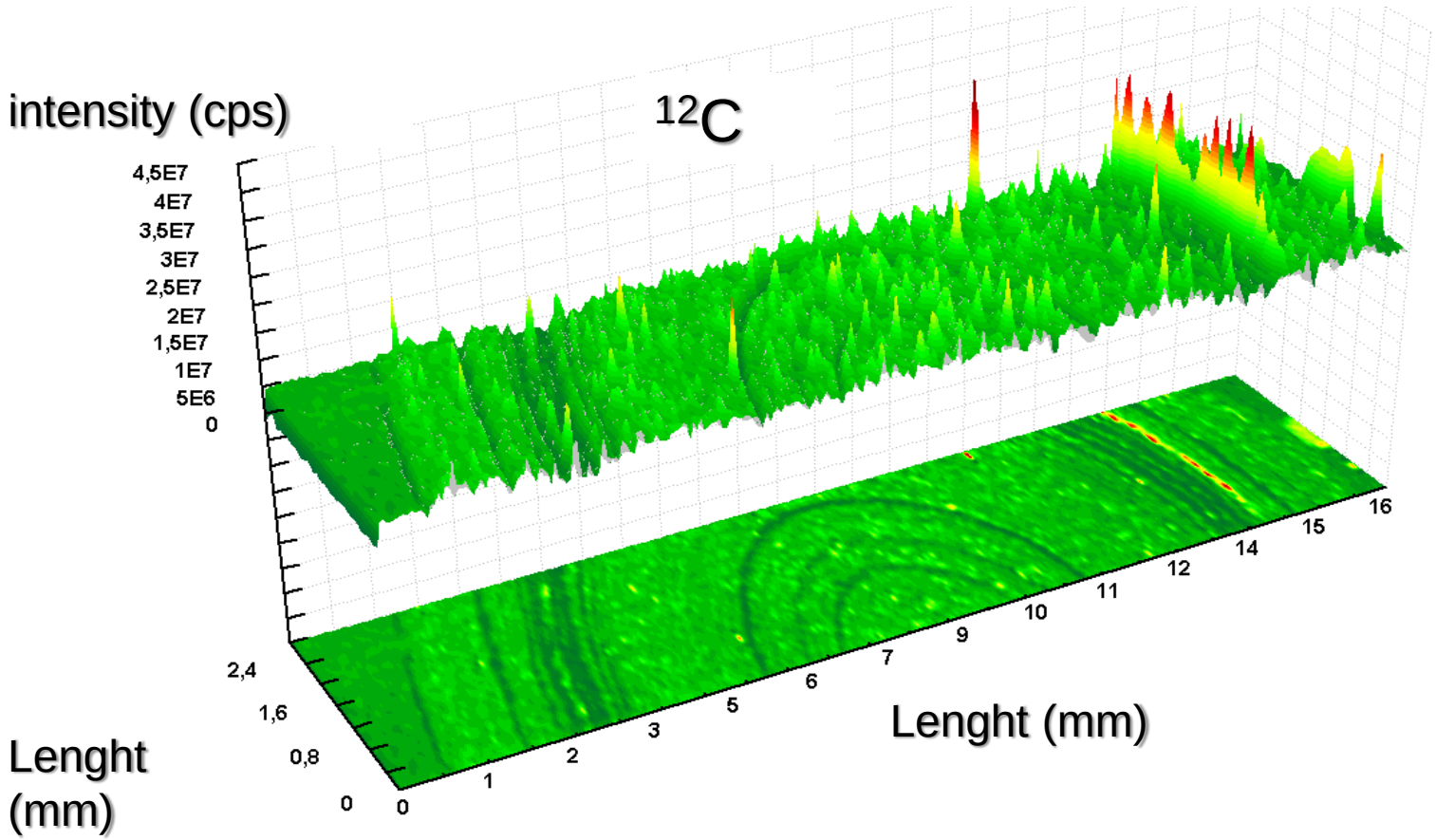

Scanned areas of uroliths

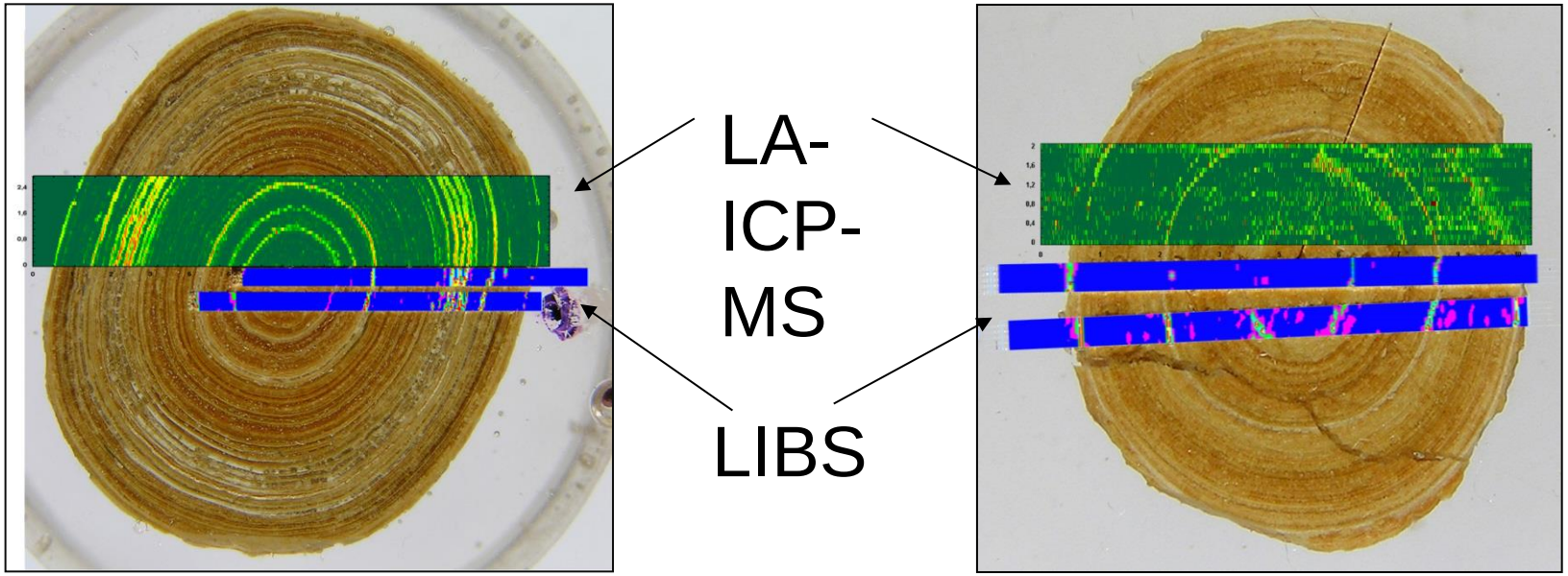

LA-ICP-MS HEAVY METAL ANALYSIS OF FISH SCALES IN SEDIMENT

- Samples - fish scales of recent fish and in the subrecent fish scales in boreholes in the oxbow lake sediments of the Morava River
- Analysis of subrecent and recent fish scales
- Study of fosilization process
- Comparison with sediment

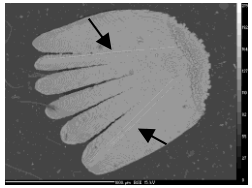

Nd:YAG laser system UP 213
line of spots with a diameter of 55 µm,
30 µm s^{-1} scan speed, 10 Hz, Fl 5 J cm^{-2}.
ICP-MS spectrometer Agilent 7500ce

Quantification on NIST 1486 (bone meal) and NIST 612 (glass)

Internal standard: Ca (EPXMA)

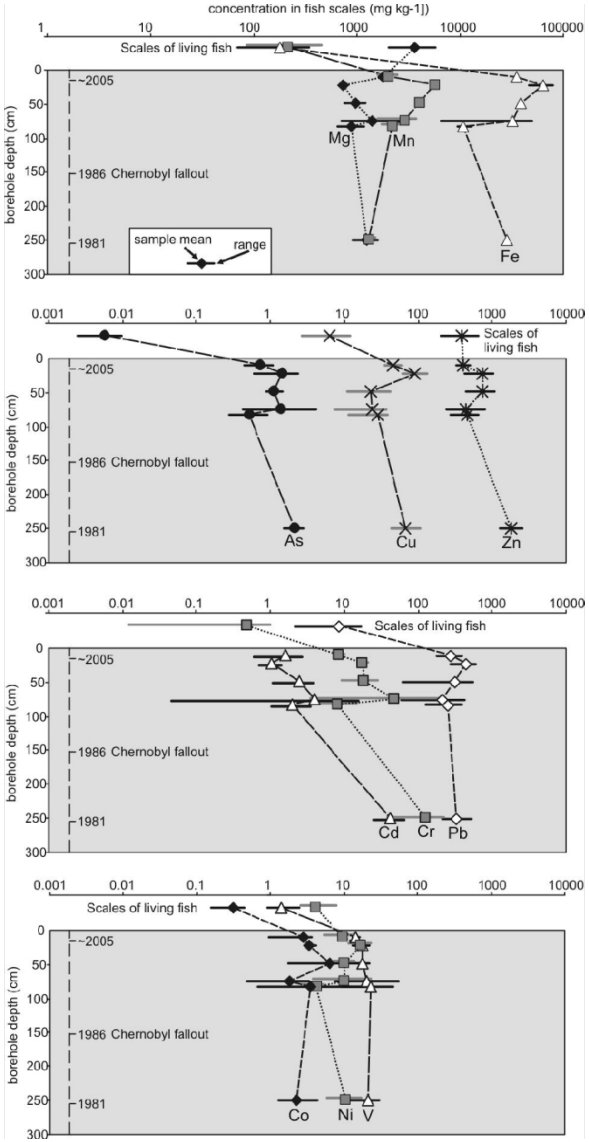

Variation in the content of the studied elements (grey lines) in fish scales of living fish and subfossil fish scales in the boreholes

The substantial loss of collagen during fossilization is very rapid and is accompanied by extremely rapid (1 to 2 years) change in the colour from white in recent fish scales to brown in subrecent ones, which is connected with the iron diffusion.

The subrecent fish scales exhibit heavy metal concentrations:

- that are an order of magnitude higher than in the recent ones
- but are similar to the concentrations found in the bulk sediment.

Markéta Holá*, Jiří Kalvoda, Ondřej Bábek, Rostislav Brzobohatý, Ivan Holoubek, Viktor Kanický, Radek Škoda

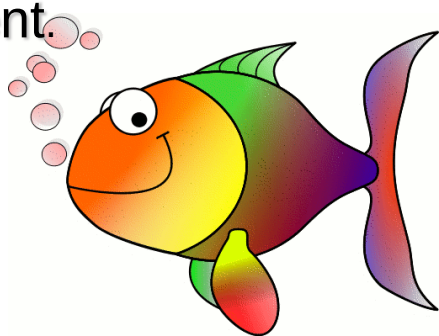

CONCLUSIONS

- LA-ICP-MS analysis of compact samples without internal standardisation is difficult but feasible.
- LIBS elemental mapping with double-pulse technique is comparable with LA-ICP-MS
- LA-ICP-MS study of history of contamination of nature
- Spatially resolved analysis of corroded surfaces by LA-ICP-MS can be complementary EPXMA
- LA-ICP-OES applicable to carbon determination